Journal Pre-proof

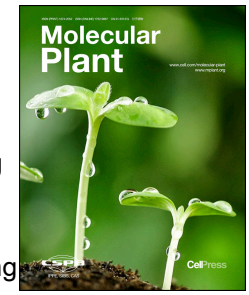

OsPRMT6a-mediated arginine methylation of OsJAZ1 regulates jasmonate signaling and spikelet development in rice

Kun Dong, Fuqing Wu, Siqi Cheng, Shuai Li, Feng Zhang, Xinxin Xing, Xin Jin, Sheng Luo, Miao Feng, Rong Miao, Yanqi Chang, Shuang Zhang, Xiaoman You, Peiran Wang, Xin Zhang, Cailin Lei, Yulong Ren, Shanshan Zhu, Xiuping Guo, Chuanyin Wu, Dong-Lei Yang, Qibing Lin, Zhijun Cheng, Jianmin Wan

PII: S1674-2052(24)00127-8

DOI: https://doi.org/10.1016/j.molp.2024.04.014

Reference: MOLP 1726

To appear in: *MOLECULAR PLANT*

Received Date: 7 December 2023

Revised Date: 4 April 2024

Accepted Date: 29 April 2024

Please cite this article as: Dong K., Wu F., Cheng S., Li S., Zhang F., Xing X., Jin X., Luo S., Feng M., Miao R., Chang Y., Zhang S., You X., Wang P., Zhang X., Lei C., Ren Y., Zhu S., Guo X., Wu C., Yang D.-L., Lin Q., Cheng Z., and Wan J. (2024). OsPRMT6a-mediated arginine methylation of OsJAZ1 regulates jasmonate signaling and spikelet development in rice. Mol. Plant. doi: https://doi.org/10.1016/j.molp.2024.04.014.

OsPRMT6a-mediated arginine methylation of OsJAZ1 regulates jasmonate signaling and spikelet development in rice

Kun Dong[1,3], Fuqing Wu[1,3], Siqi Cheng[2,3], Shuai Li[1], Feng Zhang[1], Xinxin Xing[1], Xin Jin[1], Sheng Luo[1], Miao Feng[1], Rong Miao[2], Yanqi Chang[1], Shuang Zhang[1], Xiaoman You[2], Peiran Wang[2], Xin Zhang[1], Cailin Lei[1], Yulong Ren[1], Shanshan Zhu[1], Xiuping Guo[1], Chuanyin Wu[1], Dong-Lei Yang[2], Qibing Lin[1,*], Zhijun Cheng[1,*] and Jianmin Wan[1,2,*]

[1]State Key Laboratory of Crop Gene Resources and Breeding, National Key Facility for Crop Gene Resources and Genetic Improvement, Institute of Crop Sciences, Chinese Academy of Agricultural Sciences, Beijing, 100081, China

[2]State Key Laboratory for Crop Genetics and Germplasm Enhancement, Nanjing Agricultural University, Nanjing, 210095, China

[3]These authors contributed equally to this article.

*__Corresponding author__: **Qibing Lin (**linqibing@caas.cn),

Zhijun Cheng (chengzhijun@caas.cn),

Jianmin Wan (wanjianmin@caas.cn)

Short Summary: Arginine methylation of OsJAZ1 by OsPRMT6a enhances its affinity for OsCOI1a/OsCOI1b, thus promoting the ubiquitination and degradation of OsJAZ1, finally the JA responses. In the *osprmt6a-1* mutant, the absent arginine methylation of OsJAZ1 results in the stabilization of OsJAZ1 proteins, thus repressing JA responses, finally leading to abnormal spikelet structures. Additionally, JA signaling reduced the *OsPRMT6a* mRNA level, establishing a negative feedback loop to balance JA signaling.

Abstract

Although both protein arginine methylation (PRMT) and jasmonate (JA) signaling are crucial for regulating plant development, the relationship between these processes in spikelet development control remains unclear. Here, we utilized CRISPR/Cas9 technology to generate two *OsPRMT6a* loss-of-function mutants exhibiting various abnormal spikelet structures. Additionally, we found that OsPRMT6a could methylate arginine residues in the JA signal repressors OsJAZ1 and OsJAZ7. Arginine methylation of OsJAZ1 increased the affinity of OsJAZ1 for the JA receptors OsCOI1a and OsCOI1b in the presence of jasmonates (JAs), subsequently promoting the ubiquitination of OsJAZ1 by the $SCF^{OsCOI1a/OsCOI1b}$ complex and degradation via the 26S proteasome. This process ultimately released OsMYC2, a core transcriptional regulator in the JA signaling pathway, to activate or repress JA-responsive genes, thereby maintaining normal plant (spikelet) development. However, in the *osprmt6a-1* mutant, reduced arginine methylation of OsJAZ1 impaired the interaction between OsJAZ1 and OsCOI1a/OsCOI1b in the presence of JAs. As a result, OsJAZ1 proteins became more stable, repressing JA responses, thus causing the formation of abnormal spikelet structures. Moreover, we discovered that JA signaling reduced the *OsPRMT6a* mRNA level in an OsMYC2-dependent manner, thereby establishing a negative feedback loop to balance JA signaling. Furthermore, we found that OsPRMT6a-mediated arginine methylation of OsJAZ1 likely serves as a switch to tune JA signaling to maintain normal spikelet development under harsh environmental conditions such as high temperatures. Thus, our study established a direct molecular link between arginine methylation and the JA signaling pathway.

Keywords: protein arginine methylation, jasmonate signaling, negative feedback loop, spikelet development, adaptation to heat stress, rice

Introduction

Jasmonates (JAs), comprising jasmonic acid and its volatile ester derivative methyl-jasmonate (MeJA) and amino acid derivatives (such as JA-Ile), are important phytohormones that not only mediate plant defense responses to pathogens, herbivores, and abiotic stresses but also regulate plant growth and developmental processes such as sexual reproduction, root elongation, carbohydrate accumulation, floret development, and fruit ripening (Acosta et al., 2009; Browse and Howe, 2008; Chico et al., 2020; Chung and Howe, 2009; Goossens et al., 2017; Guo et al., 2018; Hori et al., 2014; Hu et al., 2023; Huang et al., 2017; Kim et al., 2009; Lee et al., 2013; Pauwels et al., 2008; Yoshida et al., 2009b). The JA biosynthesis and signaling pathways in rice (*Oryza sativa L.*) and Arabidopsis (*Arabidopsis thaliana*) have been well established. In JA signaling in Arabidopsis and rice, the JA receptor Coronatine-Insensitive 1 (COI1) and OsCOI1a/OsCOI1b are F-box proteins that bind to S-phase kinase-associated protein 1 (Skp1), Cullin and Rbx1 proteins to form the SCF^{COI1} E3 ubiquitin ligase complex (Devoto et al., 2002; Xu et al., 2002; Yang et al., 2012). The jasmonate ZIM domain (JAZ) proteins (comprising 12 members) and OsJAZs (comprising 15 members, OsJAZ1 to OsJAZ15) belong to the TIFY family, which is unique to plants, and function as repressors of the JA signaling pathway (Chini et al., 2007; Thines et al., 2007; Ye et al., 2009). The basic-helix-loop-helix (bHLH) transcription factor (TF) MYC2 and its homolog OsMYC2 are master regulators of most aspects of the JA signaling pathway. In the absence of JAs, JAZs/OsJAZs bind to MYC2/OsMYC2 to inhibit JA responses (Cai et al., 2014; Dombrecht et al., 2007). However, in the presence of JAs, JAZs/OsJAZs bind to the receptors COI1/OsCOI1a/OsCOI1b, promoting the binding of the $SCF^{COI1/OsCOI1a/OsCOI1b}$ complex to JAZs/OsJAZs for ubiquitination, after which the ubiquitinated JAZs/OsJAZs are degraded by the 26S proteasome (Cai et al., 2014; Cao et al., 2021; Feng et al., 2020; He et al., 2020; Sheard et al., 2010; Wu et al., 2015; Xu et al., 2002;

Yamada et al., 2012; Ye et al., 2009), thus releasing MYC2/OsMYC2 to activate or repress downstream JA-responsive genes (Chung and Howe, 2009). The genes activated by MYC2 include *VEGETATIVE STORAGE PROTEIN* (*VSP)* and *LIPOXYGENASE 3* (*LOX3*), which are involved in the injury response in Arabidopsis, and the genes activated by OsMYC2 include spikelet development-related genes such as *OsMADS1*, *OsMADS7* and *OsMADS14* in rice, while the genes repressed by MYC2 include *PATHOGENESIS-RELATED 1 (PR1),* the defense gene *PLANT DEFENSIN 1.2* (*PDF1.2),* the stress-related gene *CHITINASE B* (*CHIB*)*, and PATHOGENESIS-RELATED 4 (PR4)* (Brown et al., 2003; Chen et al., 2006; Cheong et al., 2002; Lorenzo et al., 2004; Reymond et al., 2000; You et al., 2019).

In grasses, the spikelet is the fundamental unit of inflorescence structure, consisting of rudimentary glumes and sterile lemmas, as well as a single fertile floret comprising a lemma, a palea, two lodicules, six stamens, and one pistil (Yoshida and Nagato, 2011). Spikelet development is crucial for the formation of inflorescence structure and grain yield. Many genes that control rice spikelet development, such as *LONG STERILE LEMMA* (*ELE*, *G1)*, *MULTI-FLORET SPIKELET 1 (MFS1)*, *OSINDETERMINATE SPIKELET 1 (OsIDS1)*, *OsMADS1*, *OsMADS7*, and *OsMADS14*, have been identified (Chen et al., 2006; Cui et al., 2010; Jeon et al., 2000; Komatsu et al., 2003; Lee and An, 2012; Lee et al., 2007; Lim et al., 2000; Malcomber and Kellogg, 2004; Ren et al., 2013; Yoshida et al., 2009a; Zhang et al., 2017). In addition to regulating defense responses, JA signaling also regulates spikelet development in plants. For instance, abnormal spikelet morphology has been observed in mutants with loss of function of genes related to JA synthesis, such as *EXTRA GLUME1 (EG1)* and *OSPEROXIN 5 (OsPEX5)* (Cui et al., 2010; Li et al., 2009; Lim et al., 2000; You et al., 2019). Additionally, abnormal spikelet development has been observed upon ectopic expression of the OsJAZ JA signaling repressors (Cai et al., 2014; Cao et al., 2021; Hori et al., 2014). Notably, JA signaling can shape spikelet morphology through OsMYC2-mediated regulation of *OsMADS1*, *OsMADS7* and *OsMADS14*

(Chen et al., 2006; You et al., 2019).

Protein arginine methylation is a common and significant posttranslational modification (PTM) in eukaryotes that plays a crucial role in various biological processes, including transcriptional regulation, chromatin remodeling, RNA metabolism, protein nucleocytoplasmic translocation, signal transduction, and apoptosis (Bedford and Clarke, 2009; Blanc and Richard, 2017). Protein arginine methylation is enzymatically catalyzed by a family of proteins known as protein arginine methyltransferases (PRMTs), which methylate histones and a wide array of nonhistone proteins (Bedford and Clarke, 2009). PRMTs facilitate the transfer of methyl groups from S-adenosyl-L-methionine (SAM) to arginine residues within target proteins. Depending on the position and number of methyl groups attached to the ω-guanidine nitrogen atom of arginine, arginine methylation can be categorized into three types: monomethylarginine (MMA), symmetric dimethylarginine (SDMA), and asymmetric dimethylarginine (ADMA) (Wolf, 2009).

PRMTs are widely distributed in single-celled organisms, eukaryotic yeasts, higher animals, and plants. Humans harbor 11 members of the PRMT family: PRMT1 to PRMT11. They all possess conserved catalytic functional domains, including motifs I, post-I, II, and III, the "double E motif," and the THW (Thr-His-Trp) loop (Cheng et al., 2005). Most research on arginine methyltransferases in higher plants has been carried out in Arabidopsis, with only limited studies in rice. *Arabidopsis thaliana* contains 9 homologous PRMT proteins. Among these proteins, AtPRMT1a and AtPRMT1b, which are homologs of human PRMT1, synergistically and asymmetrically dimethylate histone H4, H2A, myelin basic protein, and AtFib2 (Yan et al., 2007). In planta research has shown that AtPRMT3 deficiency results in an imbalance and abnormalities in the pre-rRNA processing pathway (Hang et al., 2014). AtPRMT4a, AtPRMT4b, AtPRMT5, AtPRMT10 and AtPRMT11 participate in regulating flowering in Arabidopsis (Hong et al., 2010; Pei et al., 2007; Schmitz et al., 2008; Wang et al., 2007), and an *atprmt11* mutant exhibited abnormal inflorescence morphology with several sterile florets (Scebba et al., 2007).

123 *Oryza sativa* has eight homologous PRMT proteins, OsPRMT1, OsPRMT3, OsPRMT4,
124 OsPRMT5, OsPRMT6a, OsPRMT6b, OsPRMT7, and OsPRMT10, and although their
125 methylation activities have been confirmed *in vitro*, their specific substrates and biological
126 functions in planta are still poorly understood (Ahmad et al., 2011). In particular, the biological
127 functions of AtPRMT6 in Arabidopsis and of OsPRMT6a and OsPRMT6b in rice remain unclear.
128 Here, we found that loss of OsPRMT6a function leads to abnormal spikelet morphology.
129 OsPRMT6a methylates the arginine residues of OsJAZ1. Arginine-methylated OsJAZ1 has a
130 stronger affinity for OsCOI1a/OsCOI1b, thus facilitating the ubiquitination of OsJAZ1 by the
131 $SCF^{OsCOI1a/OsCOI1b}$ complex and the subsequent degradation of ubiquitinated OsJAZ1 by the 26S
132 proteasome. This mechanism enables the effective transmission of JA signaling, which is crucial
133 for proper spikelet development. Additionally, MeJA downregulates the mRNA level of
134 *OsPRMT6a* through OsMYC2 via a negative feedback loop. Thus, our study established a direct
135 link between protein arginine methylation and JA signaling, a relationship critical for rice spikelet
136 development.
137

138 Results

139 *OsPRMT6a* mutation causes abnormal spikelet morphology

140 To elucidate the developmental biology of rice spikelets, we utilized CRISPR/Cas9 technology
141 to construct a mutant library from which two mutants with abnormal spikelet morphology were
142 isolated. Sequencing analysis revealed a 1 bp deletion in the *osprmt6a-1* mutant and a 1 bp
143 insertion in the *osprmt6a-2* mutant within the *OsPRMT6a* (Os10g0489100) gene **(Fig. 1A**).
144 Compared to the wild type (WT), both mutants exhibited various abnormal spikelet structures,

145 ranging from nearly normal structures to those with extreme deformities, including long sterile
146 lemma, long sterile lemma, and spikelet-like structures, eight stamens, three stigmas and
147 stamen-like organs, and other deviations **(Fig. 1B-1U**, **Supplementary Table 1**). Scanning
148 electron micrographs of spikelets at early stages Sp5 to Sp6 in *osprmt6a-1* revealed bulging
149 floral meristems, abnormal sterile lemma, ectopic stamen-like structures, and irregular glume-
150 like structures **(Supplementary Fig. 1**). Additionally, the two mutants exhibited atypical
151 agronomic traits, such as shorter plant height, increased tiller number, lower seed setting rate,
152 and altered panicle type and grain size **(Supplementary Fig. 2**).

153 To confirm that the *OsPRMT6a* mutation caused these phenotypes, we performed RNA
154 interference (RNAi) analysis and a transgenic complementation test. The results showed that
155 the phenotypes of the *OsPRMT6a*-RNAi lines (Ri1 and Ri2) mirrored those of *osprmt6a-1* and
156 *osprmt6a-2*, while those of the complement transgenic line resembled those of the WT
157 **(Supplementary Fig. 3**), confirming that the *osprmt6a-1* and *osprmt6a-2* mutant phenotypes
158 were caused by mutations in *OsPRMT6a*. Given the similar phenotypes of *osprmt6a-1* and
159 *osprmt6a-2*, we exclusively utilized *osprmt6a-1* in subsequent experiments.

160 Phylogenetic and protein sequence analyses revealed that OsPRMT6a is a typical protein
161 arginine methyltransferase with conserved PRMT signature motifs I, post-I, -II, and -III, a THW
162 loop (black bars) and a double E loop **(Supplementary Figs. 4, 5**). RT–qPCR analysis revealed
163 widespread expression of *OsPRMT6a*, with relatively high levels in leaf sheaths and panicles
164 **(Supplementary Fig. 6A**). Subcellular localization analysis of rice protoplasts revealed nuclear
165 predominance with a weak membrane distribution **(Supplementary Fig. 6B, 6C**). mRNA *in situ*
166 hybridization revealed that *OsPRMT6a* was widely expressed in the inflorescence meristem (IM),
167 primary branch meristem (PBM), secondary branch meristem (PBM), and spikelet (SP)
168 **(Supplementary Fig. 6D**-**6H**).

169 In conclusion, these results suggest that OsPRMT6a likely participates in regulating various

plant development processes, including spikelet development.

OsPRMT6a physically interacts with several OsJAZs to methylates arginine residues in OsJAZ1

To explore how OsPRMT6a regulates spikelet development, we conducted yeast two-hybrid (Y2H) library screening to identify potential substrates of OsPRMT6a. Because the abnormal spikelet morphology in *osprmt6a* closely resembles that caused by mutations in JAZ family proteins (Cai et al., 2014; Hori et al., 2014), we selected JAZ family proteins identified from the Y2H library screening as candidate OsPRMT6a substrates for use in subsequent experiments.

To investigate the interaction between OsPRMT6a and 15 members of the rice JAZ family, we performed Y2H assays and revealed that OsJAZ5, OsJAZ6, OsJAZ7 and OsJAZ8 physically interact with OsPRMT6a **(Supplementary Fig. 7**). Subsequently, through *in vivo* coimmunoprecipitation (CoIP), *in vitro* pull-down, luciferase (LUC) complementation imaging and bimolecular fluorescence complementation (BiFC) assays, we confirmed that OsPRMT6a interacts with OsJAZ1, OsJAZ7, and OsJAZ8 **(Fig. 2A-2D, Supplementary Fig. 8)**.

The protein interaction analysis results suggested that some OsJAZs (OsJAZ1, OsJAZ7 and OsJAZ8) were potential OsPRMT6a substrates. To verify this, OsJAZ1 was selected as a representative protein for use in subsequent analyses due to its well-defined role in JA signaling. An *in vitro* methylation assay showed that OsJAZ1 was methylated by OsPRMT6a **(Fig. 2E**). Then, we utilized the methylated OsJAZ1 obtained via an *in vitro* methylation assay to analyze the specific methylation sites catalyzed by OsPRMT6a via mass spectrometry and ultimately identified five distinct arginine methylation sites **(Fig. 2G-2I**). Furthermore, using mass spectrometry, we analyzed the methylation of OsJAZ1-GFP proteins immunoprecipitated with an anti-GFP antibody from transgenic plants in the WT background and *osprmt6a-1* background.

193 An arginine modification site was found only in OsJAZ1-GFP from the WT, not in those from
194 *osprmt6a-1* background transgenic plants **(Supplementary Fig. 9)**, suggesting that OsJAZ1 is
195 likely methylated *in vivo* by OsPRMT6a. Using the same method, we also identified two arginine
196 methylation sites in OsJAZ7 that were modified *in vitro* by OsPRMT6a **(Supplementary Fig. 10)**.
197 To validate the five arginine methylation sites in OsJAZ1, we substituted them with lysine to
198 prevent methylation. The replacement of the 58th amino acid (an arginine methylation site
199 identified by *in vivo* IP-MASS) with one lysine is represented as "1K", and "5K" denotes the
200 replacement of all five identified arginines with lysines in OsJAZ1, mimicking the nonmethylated
201 state of the protein. An *in vitro* arginine methylation assay confirmed that OsJAZ1 (5K) had less
202 methylation catalyzed by OsPRMT6a than did OsJAZ1 and OsJAZ1 (1K) **(Fig. 2E)**, confirming
203 that the five arginines were indeed the sites of OsJAZ1 methylation catalyzed by OsPRMT6a.
204 To investigate whether OsPRMT6a methylates OsJAZ1 *in vivo*, we generated the
205 *p35S:OsJAZ1-GFP/*WT (in the WT background) and *p35S:OsJAZ1-GFP/osprmt6a-1* (in the
206 *osprmt6a-1* background) transgenic lines. Lines with similar *OsJAZ1* expression levels (L4-8 and
207 L3-1) were used for subsequent experiments **(Supplementary Fig. 11)**. OsJAZ1-GFP
208 overexpression did not affect the phenotype of the recipient plants. Notably, the *p35S:OsJAZ1-*
209 *GFP/osprmt6a-1* transgenic plants exhibited abnormal spikelet morphology similar to that of
210 *osprmt6a-1*, while *p35S:OsJAZ1-GFP/*WT transgenic plants displayed normal spikelet
211 morphology similar to that of the WT plants **(Supplementary Fig. 12)**. By detecting OsJAZ1-
212 GFP with an anti-arginine methylation antibody, we detected higher arginine methylation levels
213 of OsJAZ1-GFP in the WT plants than in the *osprmt6a-1* plants **(Fig. 2F)**. According to the
214 developmental stages of rice spikelets defined in previous research (Ikeda et al., 2004), we
215 assessed the OsJAZ1-GFP level and OsJAZ1-GFP arginine methylation levels in rice spikelets
216 from stages ln 3 to ln 9. The OsJAZ1-GFP level increased, while the OsJAZ1-GFP arginine
217 methylation level decreased, from stages In 3 to ln 6. The lowest OsJAZ1-GFP level,

accompanied by the highest arginine methylation level, occurred at stage In 7, and there was a return to lower OsJAZ1-GFP levels with reduced arginine methylation levels from stages In 8 to ln 9 **(Supplementary Fig. 13)**. According to previous research (Ikeda et al., 2004), In 6 and In 7 are two key stages in the initiation and development of spikelet organs, such as the sterile lemma, lemma, palea, and various floret organs, such as the stamen, lodicule, and carpel. Here, we observed severe downregulation of the OsJAZ1-GFP content and strong upregulation of arginine methylation in OsJAZ1-GFP between the In 6 and In 7 stages **(Supplementary Fig. 13)**, which was consistent with the abnormal spikelets and floret organs observed in the *osprmt6a* mutants.

In summary, these results demonstrate that OsJAZ1 is methylated by OsPRMT6a both *in vivo* and *in vitro*, suggesting that OsPRMT6a likely regulates spikelet development by methylating OsJAZ1.

Arginine methylation of OsJAZ1 promotes OsJAZ1 degradation

JAZs are known to serve as direct targets for the SCF^{COI1} E3 ubiquitin ligase, and the application of JAs induces the ubiquitination and degradation of JAZs (Chini et al., 2007; Xu et al., 2002). To investigate whether arginine methylation of OsJAZ1 influences JA-induced OsJAZ1 degradation, we subjected various rice seedlings to short-term treatment with different concentrations of MeJA. The results showed that both native OsJAZ1 protein and JAZ1-GFP fusion protein in the osprmt6a-1 mutant background were less susceptible to degradation than those in the WT background under MeJA treatment (**Fig 3A, 3B, Supplementary Fig. 14, 15**).

The JA content was measured, revealing that the WT and *osprmt6a-1* seedlings had much lower JA content than did their spikelets, while the WT had slightly lower JA content than did the *osprmt6a-1* mutant **(Fig. 3C).** Notably, the lower JA content in the seedlings likely led to less JA-induced degradation of OsJAZ1 and OsJAZ1-GFP, establishing a positive correlation between

the OsJAZ1/OsJAZ1-GFP levels and their mRNA levels in both the WT and *osprmt6a-1* backgrounds **(Fig. 3A-3E)**. However, in the spikelets, a greater JA content triggered substantial degradation of OsJAZ1 and OsJAZ1-GFP in the WT background but not in the *osprmt6a-1* background. This reduced the OsJAZ1 and OsJAZ1-GFP levels in the WT background compared to those in the *osprmt6a-1* background, despite the higher *OsJAZ1* mRNA levels in the WT background than in the *osprmt6a-1* background **(Fig. 3D, 3E)**.

To assess the impact of the modification status of the five identified arginine methylation sites on protein stability, we conducted a dual-LUC degradation assay to compare the stabilities of the OsJAZ1 (5K) and OsJAZ1 proteins. Plasmids expressing the OsJAZ1 (5K)-LUC and OsJAZ1-LUC fusion proteins were constructed and transfected into *Nicotiana benthamiana* leaves. The “LUC/REN” bioluminescence ratio was measured at 48 hours and 72 hours posttransfection. We observed accumulation of OsJAZ1 (5K) in the demethylated state, in contrast to the decreasing amount of OsJAZ1 over time **(Fig. 3F, 3G)**. Similarly, in the cell-free degradation assay, maltose-binding protein (MBP)-OsJAZ1 (5K) exhibited greater stability than MBP-OsJAZ1 over time **(Fig. 3H)**.

In conclusion, these results demonstrate that arginine methylation of OsJAZ1 by OsPRMT6a promotes OsJAZ1 degradation in rice.

Arginine methylation of OsJAZ1 promotes the interaction of OsJAZ1 with OsCOI1a and OsCOI1b, facilitating OsJAZ1 ubiquitination

JAZs are known to bind to the JA receptor COI1 in the SCF^{COI1} complex, leading to the ubiquitination and subsequent degradation of the JAZs (Xu et al., 2002). In rice, OsCOI1a and OsCOI1b, which are homologs of COI1, function as receptors for JAs (Yang et al., 2012). To

investigate whether arginine methylation of OsJAZ1 influences OsJAZ1 degradation by affecting the interaction of OsJAZ1 with OsCOI1a and OsCOI1b, we conducted the following analyses.

The interaction between COI1 and JAZ is JA dependent (Katsir et al., 2008; Sheard et al., 2010). We performed Y2H assays with coronatine (COR), a mimic of JA-Ile, in quadruple dropout (QDO) media following methods described in previous research (Cai et al., 2014). The results revealed an interaction between OsJAZ1 and OsCOI1b in the presence of COR, but no interaction was detected between OsJAZ1 and OsCOI1a **(Fig. 4A)**. Using the *p35S:OsJAZ1-GFP*/WT and *p35S:OsJAZ1-GFP/osprmt6a-1* transgenic plants, along with the MBP-tagged fusion protein MBP-OsCOI1b (since we lacked an anti-OsCOI1b antibody) expressed in a prokaryotic system, we conducted semi-*in vivo* and *in vivo* CoIP assays. OsJAZ1-GFP increased the enrichment of recombinant MBP-OsCOI1b proteins and native OsCOI1a proteins in the total protein extracts from the *p35S:OsJAZ1-GFP*/WT transgenic plants compared to the total protein extracts from the *p35S:OsJAZ1-GFP/osprmt6a-1* transgenic plants **(Fig. 4B, 4C**). Using a transient expression system in rice protoplasts for *in vivo* CoIP assays, we detected stronger interactions of OsCOI1a-Flag or OsCOI1b-Flag with OsJAZ1-GFP than with the OsJAZ1 (5K)-GFP fusion protein **(Fig. 4D, 4E)**. This finding was inconsistent with previous reports that, through BiFC and Y2H analyses, showed that OsJAZ1 and OsCOI1a could not interact (Cai et al., 2014; Cao et al., 2021). To determine the possible reasons for this inconsistency, we performed additional BiFC and luciferase complementation imaging (LCI) assays. Neither the LCI nor the BiFC assay revealed an interaction between OsCOI1a and OsJAZ1 in the absence of OsPRMT6a, as has been previously reported (Cai et al., 2014; Cao et al., 2021); however, when OsPRMT6a was coexpressed, both assays revealed an interaction **(Fig. 4F, 4G)**, indicating that the interaction between OsJAZ1 and OsCOI1a *in vivo* depends on OsPRMT6a.

OsJAZ1 suppresses JA signaling by interacting with OsMYC2 in the absence of JAs. Therefore, to assess whether the arginine methylation of OsJAZ1 affects the interaction of

OsJAZ1 with OsMYC2, a Y2H assay was performed. The results indicated that both OsJAZ1 and OsJAZ1 (5K) exhibited similar abilities to bind to OsMYC2 **(Supplementary Fig. 16)**, suggesting that arginine methylation of OsJAZ1 does not affect the interaction of OsJAZ1 with OsMYC2.

Furthermore, using the MBP-OsJAZ1 and MBP-OsJAZ1 (5K) proteins expressed in *E. coli*, we conducted an *in vitro* ubiquitination assay. The results revealed a decrease in ubiquitinated MBP-OsJAZ1 proteins in *osprmt6a-1* plant extracts or MBP-OsJAZ1 (5K) proteins in WT plant extracts compared to ubiquitinated MBP-OsJAZ1 in WT plant extracts **(Fig. 4H)**. These results indicate that the arginine methylation of OsJAZ1 by OsPRMT6a promotes the interaction of OsJAZ1 with OsCOI1a and OsCOI1b, subsequently facilitating OsJAZ1 ubiquitination.

Consistent with these findings, the *oscoi1a oscoi1b* double mutant plants also exhibited abnormal spikelet morphology similar to that observed in the *osprmt6a* plants **(Supplementary Fig. 17)**, supporting the conclusion that arginine methylation of OsJAZ1 enhances the interaction of OsJAZ1 with OsCOI1a or OsCOI1b, promoting OsJAZ1 ubiquitination and ultimately influencing spikelet development.

The stabilization of OsJAZ1 by the loss of arginine methylation impedes JA responses and normal spikelet development

In Arabidopsis, both JAZ-overexpressing and JAZ knockout plants exhibit abnormal responses to JAs (Guo et al., 2018; Yan et al., 2014). To investigate whether the stabilization of OsJAZ1 in *osprmt6a-1* leads to abnormal JA responses, we treated the WT and *osprmt6a-1* plants with 2 mM MeJA and observed the responses of the plants by analyzing the changes in the expression of JA-responsive genes. The results indicated reduced expression of these JA signaling genes in *osprmt6a-1* relative to the WT seedlings **(Fig. 5A)**, signifying diminished JA responses in

313 *osprmt6a-1* compared to the WT. For analyzing gene expression differences between the WT
314 and *osprmt6a-1* under normal conditions, we conducted a global RNA-seq analysis using RNA
315 extracted from approximately 1-cm-long inflorescences. Cluster analysis revealed differences in
316 the expression of thousands of genes, including 17 genes related to the JA signaling pathway,
317 90 genes related to ubiquitin-mediated proteolysis, and numerous other genes involved in plant
318 development **(Supplementary Data 1)**. RT−qPCR analyses confirmed significant reductions in
319 the expression of many genes related to the JA signaling pathway in *osprmt6a-1* compared to
320 that in the WT, validating the RNA-seq analysis results **(Fig. 5B, 5C)**. Together, these findings
321 support the notion that stabilized OsJAZ1 (and possibly other OsJAZs) in *osprmt6a-1* diminishes
322 JA responses in plants.

323 Previous studies have demonstrated that nondegradable JAZ variants lead to abnormal
324 spikelet development by reducing JA responses (Cai et al., 2014; Cao et al., 2021; Hori et al.,
325 2014). Therefore, to investigate whether stabilized OsJAZ1, due to the loss of arginine
326 methylation, has similar effects on spikelet development, we generated *p35S:OsJAZ1 (1K)-*
327 *GFP*/WT and *p35S:OsJAZ1 (5K)-GFP*/WT transgenic plants from the japonica rice cultivar
328 Kitaake for genetic analysis. As anticipated, the *p35S:OsJAZ1 (5K)-GFP*/WT transgenic plants
329 exhibited abnormal spikelets resembling those of *osprmt6a* plants **(Fig. 5D-5P)**, while the
330 *p35S:OsJAZ1-GFP/*WT and *p35S:OsJAZ1 (1K)-GFP*/WT transgenic plants did not exhibit any
331 abnormal phenotypes **(Supplementary Fig. 18)**, indicating that the 1K modification of OsJAZ1
332 is insufficient to mediate the regulatory effect of OsPRMT6a on spikelet development. Overall,
333 the similarity in spikelet abnormalities observed in both the *osprmt6a* and *p35S:OsJAZ1 (5K)-*
334 *GFP/*WT transgenic plants suggests that the abnormal spikelet development in *osprmt6a* likely
335 results from the absence of arginine methylation in OsJAZ1.

JA represses the expression of *OsPRMT6a* through OsMYC2

Considering the common occurrence of negative feedback in hormone regulation, we sought to investigate whether JA signaling influences the expression of *OsPRMT6a*. To explore this possibility, WT seedlings were treated with 1 mM MeJA and sampled at specific time points, after which the mRNA and protein levels were measured via RT–qPCR and Western blotting, respectively. The results revealed a reduction in both the mRNA and protein levels of *OsPRMT6a* following MeJA treatment **(Fig. 6A, 6B)**.

Subsequently, we aimed to identify the transcription factor that directly represses *OsPRMT6a* expression in response to JAs. By analyzing the promoter sequence of *OsPRMT6a* with PlantCARE, an online database of cis-acting regulatory elements in plants (Lescot et al., 2002), we identified six recognizable motifs (P1-P6) of the MYC family in the promoter and intron of *OsPRMT6a* **(Fig. 6C)**. Given that MYC2 is a crucial regulator of JA-responsive genes (Chini et al., 2007), we investigated whether OsMYC2 (the rice homolog of MYC2) could bind to the promoter of *OsPRMT6a* using a chromatin immunoprecipitation (ChIP)-qPCR assay. To express the OsMYC2-GFP fusion protein, along with the *OsPRMT6a* promoter and coding sequence, we generated two transient expression vectors and infected tobacco leaves via *Agrobacterium*-mediated transformation. The ChIP−qPCR results indicated that P2 and P3, but not P1, P4, P5 or P6, were amplified from immunoprecipitates pulled down by the anti-GFP antibody **(Fig. 6D)**. Yeast one-hybrid (Y1H) assays revealed that OsMYC2 could bind to the P2 region in the *OsPRMT6a* promoter **(Fig. 6E)**. Additionally, we conducted a DNA electrophoretic mobility shift assay (EMSA) to confirm whether OsMYC2 directly regulates *OsPRMT6a* transcription by binding to the G-box motif (5’-CACGTG-3’) of P2 *in vitro*. The results showed that the MBP - OsMYC2 fusion protein, rather than the free MBP protein, specifically bound to the DNA probe containing P2 with one G-box motif **(Fig. 6F)**. Furthermore, a LUC reporter assay demonstrated

that *OsPRMT6a* promoter-driven LUC expression was repressed by OsMYC2-GFP **(Fig. 6G, 6H)**. To genetically validate that the regulation of *OsPRMT6a* by JAs is OsMYC2 dependent, we generated a loss-of-function mutant, *osmyc2*, by CRISPR/Cas9 technology and found that the *osmyc2* mutant, similar to the *osprmt6a* mutants, also displayed abnormal spikelet structures **(Supplementary Fig. 19)**. Under 1 mM MeJA treatment, the *OsPRMT6a* mRNA level did not decrease in *osmyc2* **(Fig. 6I)**, in contrast to the reduction observed in the WT **(Fig. 6A)**. These results suggest that JAs likely repress the expression of *OsPRMT6a* through OsMYC2.

There was a negative correlation between the OsJAZ1 arginine methylation level and high temperature

After a three-year investigation of the rate of spikelet abnormality in Shunyi district, Beijing, we found that the rate of spikelet abnormality in *osprmt6a-1* in 2021 was lower than that in 2020 and 2022 **(Supplementary Table 1)**. In the Shunyi district, Beijing, the critical period for spikelet formation occurs in July. To explore whether climatic differences were responsible for the differences in the rates of spikelet abnormality in *osprmt6a-1* between 2021 and 2020 or 2022, we obtained climate data for July from a Chinese weather website (https://www.tianqi.com/). In July 2020, the average maximum and minimum temperatures were 31 °C and 22 °C, respectively, with a minimum temperature of 20 °C and 7 overcast or rainy days. In July 2022, the average maximum and minimum temperatures were 32 °C and 22 °C, respectively, with a minimum temperature of 20 °C and 6 overcast or rainy days. In contrast, in July 2021, the average maximum and minimum temperatures were 29 °C and 22 °C, respectively, with a minimum temperature of 18 °C and 18 overcast or rainy days **(Supplementary Table 2)**. These data indicated that the *osprmt6a-1* spikelet abnormalities occurred more readily on sunny days with higher temperatures than on rainy days with lower temperatures **(Supplementary Tables**

1, 2). In line with this observation, we observed a negative correlation between high temperature and both the protein level of OsPRMT6a and the arginine methylation level of OsJAZ1-GFP but a positive correlation between high temperature and the protein level of OsJAZ1-GFP in the *p35S:OsJAZ1-GFP/*WT transgenic plants; however, these dynamic changes were absent in the *p35S:OsJAZ1-GFP/osprmt6a-1* transgenic plants **(Supplementary Fig. 20A)**.

To alleviate the influence of environmental factors and circadian rhythms that likely affect JA biosynthesis and signaling (Thines et al., 2019), we planted *p35S:OsJAZ1-GFP*/WT and *p35S:OsJAZ1-GFP/osprmt6a-1* in different growth chambers (with different temperatures) and collected the spikelets at 10:00 AM. Similar results confirmed that there was indeed a negative correlation between the OsJAZ1 arginine methylation level and high temperature **(Supplementary Fig. 20B)**. Additionally, we planted the WT and *osprmt6a-1* plants in different growth chambers to mimic natural temperature changes **(Supplementary Table 4)** and observed the formation of abnormal spikelets. The results showed that mimicking a relatively high natural temperature caused a greater percentage of abnormal spikelets than did mimicking a relatively low natural normal temperature **(Supplementary Table 5)**, providing genetic evidence indicating that OsPRMT6a-mediated arginine methylation likely facilitates normal spikelet development under high-temperature conditions.

Discussion

In summary, our study revealed the pivotal role of OsPRMT6a in maintaining normal spikelet development. We propose a model in which OsPRMT6a methylates arginine residues of OsJAZ1, enhancing their interaction with the JA receptors OsCOI1a and OsCOI1b. This interaction triggers the ubiquitination and subsequent degradation of OsJAZ1, ensuring efficient JA signal transduction **(Fig. 7)**. By establishing a molecular link between JA signaling and

406 arginine methylation, our findings not only shed new light on the transduction mechanism and
407 self-balancing nature of JA signaling but also provide insights into the intricate interplay between
408 arginine methylation and key regulators of plant defense and development.

409 Previous reports have highlighted the impact of protein arginine methylation on protein
410 stability via modulation of substrate phosphorylation levels and direct effects on protein−protein
411 interactions (Bedford and Clarke, 2009; Estève et al., 2011; Fang et al., 2014; Yamagata et al.,
412 2008). Our study provides a novel perspective demonstrating that arginine methylation
413 influences protein stability. OsPRMT6a-catalyzed arginine methylation of OsJAZ1 primarily
414 affects stability by modulating the interaction of OsJAZ1 with OsCOI1a and OsCOI1b, ultimately
415 leading to ubiquitination by the $SCF^{OsCOI1a/OsCOI1b}$ complex **(Fig. 4)**. Eukaryotic proteins undergo
416 various posttranslational modifications at different stages of their functions, and these
417 modifications interact with each other to produce diverse biological effects. Previous studies
418 have emphasized the interplay between protein arginine methylation and other modifications,
419 such as phosphorylation (Carr et al., 2011; Yang et al., 2010) and acetylation (Ivanov et al.,
420 2007). Our research established a direct link between protein arginine methylation and
421 ubiquitination, providing novel insights into the intricate mechanisms of JA signaling.

422 Notably, in the absence of JAs, OsJAZ1 can still undergo arginine methylation, which does
423 not impede its binding to OsMYC2, thus maintaining its repression of JA signaling; when
424 abundant JAs are present, the arginine methylation of OsJAZ1 efficiently promotes the
425 interaction of OsJAZ1 with the $SCF^{OsCOI1a/OsCOI1b}$ complex, leading to OsJAZ1 ubiquitination and
426 degradation and ultimately the efficient transmission of the JA signal **(Figs. 2-5, Supplementary**
427 **Figs. 14-18)**. Constitutive high levels of many plant hormones are harmful to plant growth and
428 development; thus, plants utilize a variety of negative feedback mechanisms to finely tune their
429 hormonal signaling strength (Chico et al., 2020; Tong et al., 2009; Wolters and Jurgens, 2009;
430 Wu et al., 2016). Here, we also discovered that a negative feedback pathway, OsPRMT6a-

OsJAZ1-OsMYC2-*OsPRMT6a*, likely attenuates the OsPRMT6a-mediated arginine methylation of OsJAZ1 by repressing OsPRMT6a expression to tune down JA signaling **(Fig. 6)**. These findings suggest that OsPRMT6a-mediated arginine methylation likely acts as a switch to fine-tune JA signaling.

The significance of protein arginine methylation is underscored by the comprehensive abnormal phenotypes observed in loss-of-function *osprmt6a* mutants. These mutants exhibit dwarfism, increased tiller number, reduced seed setting, abnormal floret organs, disrupted seed dormancy, altered responses to various hormones, etc. **(Supplementary Fig. 2)**. These findings imply that PRMTs, particularly OsPRMT6a, may have numerous substrates that play vital roles in regulating plant growth and development. Furthermore, protein arginine methylation, by diversifying protein forms without altering the amino acid sequence, contributes to the "protein epigenetic universe," enabling intricate regulatory functions in organisms. Thus, our study provides new insights for exploring additional PRMT substrates, including those of OsPRMT6a, to unravel the complex regulatory networks governing life processes. Additionally, the well-established link between organism adaptability and protein arginine methylation (Zhang et al., 2011) and the findings of our study **(Supplementary Fig. 20, Supplementary Tables 1-5**) suggest that OsPRMT6a-mediated arginine methylation likely acts as a switch to epigenetically fine-tune JA signaling, ensuring the adaptation of rice development (including spikelet development) to harsh environmental conditions such as high temperature.

Materials and Methods

Plant materials and growth conditions

The WT (the japonica rice cultivar Kitaake) and *osprmt6a* mutants were cultivated during the natural growing season in an experimental field located in the Shunyi district of Beijing. For RT–qPCR, protein quantitative assays, and MeJA treatment assays, the WT and mutant seedlings were cultivated in climate chambers (HP1500GS, Ruihua) under long-day conditions, comprising daily cycles of 14 hours of light at 30 °C and 10 hours of darkness at 25 °C, along with 70% humidity. The light source utilized consisted of fluorescent white-light tubes (400-700 nm, 250 μmol m^{-2} s^{-1}).

The developmental stages of the rice spikelets were determined according to previously described methods (Ikeda et al., 2004).

Overlap extension PCR-based cloning

To obtain the OsJAZ1 protein variants (1K/5K), we utilized overlap extension PCR to introduce base mutation sites. To generate the *p35S:OsJAZ1* (5K)-*GFP* constructs, the primers GFP-JAZ1F and GFP-JAZ1R, along with the base mutation primer pair, were used to amplify the PCR fragment in segments. Subsequently, the complete PCR product of OsJAZ1 (5K) was amplified using the primers GFP-JAZ1F and GFP-JAZ1R, utilizing the previously segmented PCR fragment containing the base mutation sites as a template. The PCR products were cloned and inserted into the binary vector pCAMBIA1305-GFP using the In-Fusion Advantage PCR Cloning Kit (Clontech). The *p35S:OsJAZ1 (1K)-GFP, pGADT7-OsJAZ1 (5K),* and *pMalc2x-OsJAZ1 (5K)* constructs were constructed following the same method as that described above.

Vector construction and plant transformation

To generate knockout lines for *OsPRMT6a* and *OsMYC2*, an 18-bp gene-specific fragment with NGG at its 3' end was inserted into the CRISPR/Cas9 expression vector (Lei et al., 2014).

Com-OsPRMT6a lines were produced by cloning a 7-kb full-length *OsPRMT6a* gene fragment into the pCAMBIA1305.1 vector to complement the *osprmt6a* phenotype.

For *OsPRMT6a* gene knockdown, two inverted repeats of a 304-bp sequence were amplified with a primer pair and then cloned and inserted into the pCUbi1390-ΔFAD2 vector in the sense and antisense orientations using the *XhoI/KpnI* and *BamHI/XbaI* sites to create the RNAi construct *pUbi:dsRNAi-OsPRMT6a*.

To generate *OsPRMT6a*-overexpressing transgenic plants, the 1188-bp coding sequence (CDS) of *OsPRMT6a* was inserted into the *Acc65I* restriction site in the pCAMBIA1390-flag overexpression vector driven by a maize ubiquitin promoter to construct the *pCAMBIA1390-PRMT6a-flag* construct.

To construct *p35S:OSJAZ1-GFP*, the 654-bp CDS of *OsJAZ1* was amplified with primers, and the PCR products were then inserted into the binary vector pCAMBIA1305-GFP using an In-Fusion Advantage PCR Cloning Kit (Clontech). The *p35S:OsJAZ1 (5K)-GFP* constructs were also created using the same method as that described above. Finally, the *p35S:OSJAZ1-GFP* and *p35S:OsJAZ1 (5K)-GFP* constructs were introduced into the WT variety Kitaake, and the *p35S:OSJAZ1-GFP* construct was also introduced into *osprmt6a-1*.

All transgenic rice plants were generated via *Agrobacterium*-mediated transformation of rice calli, as described previously (Hiei et al., 1994). The material for the *oscoi1a oscoi1b* double mutant was provided by Dr. Dong-Lei Yang's research group at Nanjing Agricultural University.

Cytological observation

To prepare semithin sections, panicles at various developmental stages from both *osprmt6a* and WT plants were fixed using Carnoy's solution (75% alcohol, 25% acetic acid). Subsequently, the samples were dehydrated through a gradient of 30%, 50%, 70%, 85%, 90%, 95%, and 100% acetone for 15 minutes each. Following dehydration, the samples were infiltrated with 25%, 50%, and 75% resin for 3 hours, followed by the addition of pure resin for 12 hours. After incubation at 35 °C and 45 °C for 12 hours each and then at 60 °C for 48 hours, the embedded material surrounding the sample was trimmed into a trapezoid shape to facilitate sample exposure. The samples were sectioned into 1 μm slices using an ultramicrotome and mounted on glass slides. These sections were stained with 0.5% toluidine blue, washed with water, and observed under a Nikon Eclipse E80i light microscope to examine various types of young spikelets.

For scanning electron microscopy (SEM), spikelets at early developmental stages were fixed overnight at 4 °C using a 2.5% glutaraldehyde solution and processed according to previously described methods (Mou et al., 2000).

RNA extraction and RT−qPCR

Total RNA was extracted from various tissues using the ZR Plant RNA MiniPrep Kit (Zymo Research). Subsequently, 1 μg of total RNA was subjected to a 20 μl reverse transcription reaction with a PrimeScript reverse transcriptase kit (TaKaRa, Shiga, Japan). RT–qPCR analyses were conducted in an ABI 7500 real-time PCR system with a SYBR Premix Ex Taq Kit (TaKaRa, Shiga, Japan). The rice ubiquitin gene (UBQ, Os03g0234200) served as a reference gene for normalization. The $2^{-\Delta\Delta CT}$ method was applied to analyze the relative gene expression levels. The sequences of the primers utilized in this assay and subsequent assays are listed in **Supplementary Table 4**.

Statistical analysis

Student's *t* test was used for comparing the means of two independent groups. Fisher's least significant difference (LSD) test was used for multiple mean comparisons.

RNA *in situ* hybridization

A 247-bp gene-specific cDNA fragment containing the *OsPRMT6a* coding sequence was amplified, cloned and inserted into the pGEM-T Easy vector (Promega). RNA *in situ* hybridization was conducted following a previously described procedure (Li et al., 2011).

Subcellular localization

To ascertain the subcellular localization of the OsPRMT6a protein, the coding region of *OsPRMT6a* spanning 1188 base pairs was fused upstream of green fluorescent protein (GFP) in the transient expression vector pAN580, employing the *XbaI* and *BamHI* restriction sites. The resulting construct, PAN580-6A, was driven by the double CaMV35S promoter. Using an established protocol (Cai et al., 2014), rice protoplasts were transfected with the PAN580-6A plasmid to examine the localization of the OsPRMT6a protein within the cell. GFP fluorescence was observed using a confocal laser scanning microscope (LSM 980; Zeiss).

Phylogenetic analysis and homologous sequence alignment

We performed a phylogenetic analysis using the protein sequences of all known PRMTs from Arabidopsis and rice. Additionally, the protein sequences of OsPRMT6a orthologs found in 23 other species, selected based on an E-value threshold of less than $1e^{-180}$, were retrieved from

the National Center for Biotechnology Information (NCBI) database (https://www.ncbi.nlm.nih.gov/). A phylogenetic tree with 1000 bootstrap replicates was constructed using the neighbor-joining method implemented in MEGA 11.0.10 software. Subsequently, the phylogenetic tree was refined using the EvolView website (http://www.evolgenius.info/evolview.html).

The protein sequences used for sequence alignment included OsPRMT6a and OSPRMT6b from *Oryza sativa*, AtPRMT6 from *Arabidopsis thaliana*, BRADI3g29470 from *Brachypodium distachyon*, SORBI3001G211900 from *Sorghum bicolor*, and GRMZM2G160752 from *Zea mays*. Sequence alignment was performed using BioEdit software.

Yeast two-hybrid (Y2H) assay

The GAL4 binding domain was utilized to fuse the coding sequences of *OsPRMT6a*, *OsMYC2*, and *OsCOI1b* into the *EcoRI* and *BamHI* restriction sites of the pGBKT7 vector, which was designated the "bait" vector. A cDNA library from young rice inflorescences was screened using a Y2H assay, and positive clones were identified by sequencing. The coding regions of 15 members of the rice JAZ family were inserted into the *EcoRI* and *BamHI* restriction sites of the pGADT7 vector from Clontech, designated the "prey" vector. Negative controls were established using the empty pGBKT7 and pGADT7 vectors. The Yeast Protocols Handbook (Clontech) was consulted for detailed experimental procedures.

Protein electrophoresis and Western blotting

Denatured proteins were then separated on SDS–PAGE gels and detected using antibodies through Western blotting analysis. The detailed methods used were previously described (Lin et

559 al., 2012; Zhou et al., 2013).

560 For Western blotting analysis, we selected HSP82 as the internal standard to ensure
561 consistent protein loading across different samples. The quantification of the Western blotting
562 bands was performed with the image analysis software ImageJ (Taylor et al., 2013). Images
563 were obtained with a ChemiDoc™ MP Imaging System (Bio-Rad) or Model 2800 (LI-COR).

564 Antibody preparation

565 To detect OsJAZ1, the full-length coding region of *OsJAZ1* was amplified, cloned and inserted
566 into the PGEX-4T-AB1 vector **(Supplementary Table 5)**. The resulting protein, GST-OsJAZ1,
567 was expressed in *E. coli* BL21 (DE3, TransGen) cells and subjected to affinity purification. The
568 recombinant protein was then used to generate polyclonal antibodies against OsJAZ1 in rabbits
569 (ABclonal).

570 *In vivo* coimmunoprecipitation (CoIP) assay

571 The p35S:OSJAZ1-GFP vector was utilized for the *in vivo* CoIP assay. The full-length coding
572 regions of *OsJAZ7* and *OsJAZ8* were separately cloned and inserted into the pCAMBIA1305-
573 GFP vector to produce *p35S:OsJAZ1-GFP (5K), p35S:OsJAZ7-GFP* and *p35S:JAZ8-GFP*,
574 respectively. The full-length coding region of *OsPRMT6a* was inserted into the pCUbi1390 vector
575 to produce *pUbi:OsPRMT6a-Flag*. The plasmids were then transiently expressed in *N.*
576 *benthamiana* leaves via *Agrobacterium*-mediated transfection. or in rice protoplasts.

577 Total protein extracts from *p35S:OsJAZ1-GFP*/WT and *p35S:OsJAZ1-GFP/osprmt6a-1*
578 transgenic rice plants were prepared for the cell-free *in vivo* CoIP assay. Magnetic anti-GFP
579 mAb beads (D153-11, Medical Biological Laboratories) were utilized for the immunoprecipitation
580 of OsJAZ1-GFP fusion proteins, which resulted in the enrichment of native OsCOI1a proteins or

MBP-OsCOI1b fusion proteins.

The detailed methods used for protein extraction and immunoprecipitation have been previously described (Zhou et al., 2013). Proteins were subsequently separated on 10% SDS−PAGE gels and detected using an anti-GFP antibody (598-7, Medical Biological Laboratories, 1:5000), an anti-Flag antibody (M185-7, Medical Biological Laboratories, 1:5000) and an anti-OsCOI1a antibody (AbP80385-A-SE, Beijing Protein Innovation Co., 1:1000) through Western blotting analysis.

Prokaryotic protein expression

To generate MBP and His tag fusion proteins, the full-length coding regions of *OsJAZ1*, *OsJAZ1 (1K)*, *OsJAZ1 (5K)*, *OsJAZ7*, *OsMYC2* and *OsCOI1b* were amplified, cloned and inserted into the vector pMalc2x. Among the proteins that were generated, the OsJAZ1 (1K) and OsJAZ1 (5K) proteins were mimics of the demethylated OsJAZ1 protein. The coding sequences of OsJAZ1 (1K) and OsJAZ1 (5K) were generated via base substitution, as described above. The coding region of *OsPRMT6a* was also amplified, cloned and inserted into the vector pET28a. Subsequently, the proteins MBP-OsJAZ1, MBP-OsJAZ1 (1K), MBP-OsJAZ1 (5K), MBP-OsJAZ7, MBP-OsCOI1b, MBP-OsMYC2 and MBP were expressed in cells of the *E. coli* strain BL21 (DE3, TransGen) induced with 0.1 mM isopropyl-b-D-thiogalactoside (IPTG), shaken at 16 °C for 18 h, and purified using amylose resin (E8021S, New England Biolabs). The His-PRMT6a protein was expressed under induction with 1 mM IPTG followed by cell growth with shaking at 18 °C for 18 h. The protein was then purified by using IDA-Nickel (70501-100, BEAVER). The detailed methods used for protein purification have been previously described (Duan et al., 2019).

In vitro pull-down assay

His-OsPRMT6a was used as bait to pull down approximately equal amounts of MBP, MBP-OsJAZ1, MBP-OsJAZ1 (1K), MBP-OsJAZ1 (5K) and MBP-OsJAZ7 with amylose resin (E8021S, New England Biolabs). Anti-MBP (E8032S, New England Biolabs, 1:5000) and anti-His (D291-7, Medical Biological Laboratories, 1:5000) antibodies were utilized to detect the proteins. The detailed methods used for the *in vitro* pull-down assay have been previously described (Zhou et al., 2013).

Luciferase complementation imaging (LCI) assay

The coding region of *OsPRMT6a* was fused to pCAMBIA1300-nLUC, and the coding regions of *OsJAZ1*, *OsJAZ7* and *OsJAZ8* and *OsCOI1a* were fused to pCAMBIA1300-cLUC vectors. The empty vectors pCAMBIA1300-nLUC and pCAMBIA1300-cLUC were used as negative controls. The plasmids were transiently coexpressed in *N. benthamiana* leaves via *Agrobacterium*-mediated transfection. The injected leaves were sprayed with 10 mM beetle luciferin (Promega, E1602) and placed in darkness for 3 min before luminescence detection. Then, LUC images were captured by a charge-coupled device (CCD) imaging apparatus (Berthold, LB985).

Bimolecular fluorescence complementation (BiFC) assay

The coding regions of *OsJAZ1* were fused to YNE of the p2YN vector. The coding regions of *OsCOI1a* and *OsPRMT6a* were fused to YCE of the p2YC vector. The plasmids were transiently coexpressed in *N. benthamiana* leaves via *Agrobacterium*-mediated transfection. Fluorescence signals were detected using a confocal microscope (ZEISS LSM880). The detailed methods have been previously described (Waadt and Kudla, 2008).

In vitro methylation assay

The prokaryotically expressed protein His-OsPRMT6a was incubated separately with MBP-OsJAZ1, MBP-OsJAZ1 (1K) and MBP-OsJAZ1 (5K) for 4 h at 4 °C in a reaction mixture containing MTS buffer (20 mM Tris, pH 7.5; 200 mM NaCl; 0.4 mM EDTA). The proteins were then separated by 10% SDS–PAGE and detected by Western blotting analysis using anti-methylarginine antibodies (#8015, #13222, #13522; Cell Signaling Technology, 1:1000). The protein OsJAZ1 modified by arginine methylation, which was obtained through an *in vitro* methylation assay, was also subjected to mass spectrometry analysis. The details of the methods have been previously described (Blifernez et al., 2011; Lucher and Lego, 1989).

In vivo methylation detection assay

Fifteen-day-old rice seedlings of the *p35S:OsJAZ1-GFP/*WT and *p35S:OsJAZ1-GFP/osprmt6a-1* transgenic lines were frozen in liquid nitrogen and ground to powder. Total protein was extracted from fresh powder of seedlings in triple volumes of NB1 buffer (50 mM Tris-MES, pH 8.0; 1 mM MgCl2; 0.5 M sucrose; 10 mM EDTA; 5 mM DTT) containing a proteinase inhibitor cocktail (Roche, 04693132001). The denatured proteins (95 °C, 5 minutes) were then separated on 10% SDS–PAGE gels and detected by Western blotting analysis using anti-methylarginine antibodies (#8015, #13222, and #13522; Cell Signaling Technology, 1:1000), with anti-OsJAZ1 (ABclonal, 1:1000) and anti-HSP82 antibodies (AbM51099–31-PU; Beijing Protein Innovation, 1:5000) used as loading controls.

In vivo degradation assay

Fifteen-day-old rice seedlings of the WT, *osprmt6a-1*, *p35S:OsJAZ1-GFP*/WT, *p35S:OsJAZ1-GFP/osprmt6a-1*, and *pCAMBIA1390-OsPRMT6a-Flag* transgenic plants were treated with a specific concentration of MeJA, and the seedlings were collected at specific time points. To prevent protein degradation, the seedlings were pretreated with 40 μM MG132 (Calbiochem) for 3 h. The details of the subsequent experimental procedures were as described above (Zhou et al., 2013).

Analysis of OsJAZ1-GFP and arginine methylation levels during rice spikelet development

We collected rice spikelets in the field in Shunyi district (Beijing) from the tillering stage and booting stage to the heading stage and stored them in liquid nitrogen. The collected spikelets were divided into different developmental stages according to inflorescence length and morphology as defined by Ikeda et al. (2004): In 3-5 (⩽0.9 mm long inflorescence with hairs: stage In 3, primary branch formation, 0.2-0.4 mm long; In 4, elongation of primary branches, 0.4-0.6 mm long inflorescence length; In 5, formation of high-order branches, 0.6-0.9 mm long inflorescence length); stage In 6 (differentiation of glumes, 0.9-1.5 mm long inflorescence with looming spikelet); In 7 (differentiation of floral organs, 1.5-40 mm long inflorescence with clearly visible spikelet); In 8 (rapid elongation of rachis and branches, 40-220 mm long inflorescence length); and In 9 (heading and flowering, ⩾ 220 mm long inflorescence length).

For Western blotting analysis, we used HSP82 as the internal control to ensure consistent protein loading across different samples. “OsJAZ1-GFP/HSP82” represents the relative OsJAZ1-GFP content per unit of spikelet fresh weight. “Methyl/(OsJAZ1-GFP/HSP82)” represents the relative arginine methylation level per unit of OsJAZ1-GFP. HSP82 was used as an internal control to quantify the relative protein content of OsJAZ1-GFP in different samples

668 so that the relative arginine methylation levels between different samples could be compared.

669 *In vivo* dual-luciferase (LUC) degradation assay

670 To investigate the difference in the degradation levels of the two proteins, OsJAZ1 and OsJAZ1
671 (5K), the 651-bp coding region (excluding the stop codon) of OsJAZ1/OsJAZ1 (5K) under the
672 control of the CaMV35S promoter was inserted into the *NcoI* restriction site upstream of LUC in
673 the transient expression vector pGreenll 0800-LUC to construct *p35S:OsJAZ1-LUC* and
674 *p35S:OsJAZ1 (5K)-LUC.* The plasmids for these constructs were transiently expressed in *N.*
675 *benthamiana* leaves via *Agrobacterium*-mediated transfection. Leaf samples were collected at
676 48 hours and 72 hours postinfection. The collected fresh tissue was frozen in liquid nitrogen and
677 ground to powder. Total protein was extracted from freshly harvested leaves in triple volumes of
678 NB1 buffer (50 mM Tris-MES, pH 8.0; 1 mM MgCl2; 0.5 M sucrose; 10 mM EDTA; 5 mM DTT)
679 containing a proteinase inhibitor cocktail (Roche, 04693132001). LUC activity was measured
680 using the Dual-LUC Reporter Assay System (Promega, E2920). The Dual-Glo® Luciferase
681 Assay System (Promega) was used for measuring LUC activity.
682

683 Cell-free degradation assay

684 Fresh tissues from 15-day-old *p35S:OsJAZ1-GFP/*WT and *p35S:OsJAZ1-GFP/osprmt6a-1*
685 transgenic plants were ground and pulverized to extract total protein in degradation buffer (Lin
686 et al., 2012; Wang et al., 2009). The *E. coli*-expressed fusion proteins MBP-OsJAZ1 and MBP-
687 OsJAZ1 (5K) were separately added to the total plant proteins, and the mixture was sampled at
688 0, 0.5 and 1 hours. Subsequently, MG132 (Calbiochem) was selectively added for various *in*
689 *vitro* degradation assays as indicated. Denatured proteins (95 °C, 5 minutes) were separated by
690 10% SDS–PAGE and detected by Western blotting analysis using an anti-MBP antibody. The

691 methods used have been previously described (Lin et al., 2012).

692 Semi-*in vivo* CoIP assay

693 Total protein extracts were prepared from the *p35S:OsJAZ1-GFP/*WT and *p35S:OsJAZ1-*
694 *GFP/osprmt6a-1* transgenic plants as described for the cell-free degradation assay. Purified
695 MBP-OsCOI1b fusion proteins (approximately 1 μg) were fixed to anti-GFP mAb magnetic beads
696 and incubated in 400 μl of plant extract in the presence of a protease inhibitor cocktail (Roche).
697 The mixture was gently shaken at 28 °C for 30 min. The subsequent steps mirrored those of the
698 *in vivo* COIP assay. Western blotting analysis was performed using anti-MBP or anti-GFP
699 antibodies. The methods used have been previously described (Lin et al., 2012).

700 *In vitro* ubiquitination assay.

701 The purified MBP-OsJAZ1 protein bound to amylose resin (NEB) was incubated at 28 °C with
702 equal amounts of rice seedling crude extract in binding buffer. The details of the methods used
703 have been previously described (Lin et al., 2012). The supernatants containing OsJAZ1 or
704 OsJAZ1-(Ub)n were then separated by 10% SDS–PAGE and detected by Western blotting
705 analysis using an anti-MBP antibody.

706 RNA-seq analysis

707 Total RNA was extracted from approximately 1-cm-long inflorescences, and quality (integrity)
708 was assessed using an Agilent 2100 Bioanalyzer. Only RNA samples with an RNA integrity
709 number (RIN) greater than 7 were utilized for subsequent analyses.

710 Following sample quality assessment, mRNA enrichment was performed using magnetic
711 beads with oligo (dT) sequences, which bind to the poly (A) tail of mRNA through A-T

complementary pairing. Subsequently, mRNA was fragmented using fragmentation buffer, and one-strand cDNA was synthesized with six-base random hexamers as primers. Double-stranded cDNA was generated via the addition of a buffer, dNTPs, and DNA polymerase I and was subsequently purified using AMPure XP beads. The purified double-stranded cDNA was subjected to end repair, A-tailing, and sequencing adapter ligation. Size selection was performed using AMPure XP beads, followed by PCR enrichment to construct the final cDNA library.

After library construction, the initial quantification was performed using a Qubit 2.0. The library was diluted to 1 ng/μl, and the insert size was assessed using an Agilent 2100 to ensure that it met the expected size range. Subsequently, the library's effective concentration was accurately quantified using qPCR to guarantee that the concentration exceeded 2 nM, ensuring library quality. Once the libraries were subjected to quality control, different libraries were pooled based on their effective concentrations and the desired target data volume for HiSeq sequencing.

The raw sequencing data were preprocessed to remove adapter sequences and low-quality bases using Trimmomatic. Cleaned reads were aligned to the *Oryza sativa* reference genome (RAP, The Rice Annotation Project). Gene expression levels were quantified using StringTie, and differential gene expression analysis was performed with DESeq2. Functional annotation and pathway analysis of differentially expressed genes (DEGs) were conducted using the Gene Ontology (GO) and Kyoto Encyclopedia of Genes and Genomes (KEGG) databases.

Electrophoretic mobility shift assay (EMSA)

Biotin-labeled DNA probes were synthesized by Invitrogen. A Light-Shift Chemiluminescent EMSA Kit (Thermo Fisher, 20148) was utilized according to the manufacturer's instructions. The details of the methods used have been previously described (Duan et al., 2019).

Yeast one-hybrid (Y1H) assay.

The full-length coding region of *OsMYC2* was cloned and inserted into the pB42AD vector at the *EcoRI* restriction site to obtain the *pB42AD-OsMYC2* construct. To investigate promoter activity, the full 2.2 kb region and various truncated versions of the *OsPRMT6a* promoter were amplified using primers and inserted into the *XhoI* restriction site of the pLacZi reporter vector. The resulting constructs were subsequently cotransformed into the yeast strain EGY48. The empty pB42AD vector combined with the *LacZ* reporter construct was used as a negative control. The details of the methods used have been previously described (Duan et al., 2019).

Dual-luciferase (LUC) transient reporter gene assay

The 2.2-kb promoter region of *OsPRMT6a* was amplified, cloned and inserted into the pGreenII 0800-LUC vector (Zhou et al., 2013) to generate the *pGreenII 0800-pro6A-LUC* reporter construct. The full-length coding sequence of *OsMYC2* was amplified, cloned and inserted into the pCAMBIA1305-GFP vector to generate the *p35S:OsMYC2-GFP* effector construct, while the empty pCAMBIA1305-GFP vector was used as the negative control. The plasmids were transiently expressed in *N. benthamiana* leaves via *Agrobacterium*-mediated transfection. LUC and REN activities were analyzed using a dual-luciferase reporter kit following the manufacturer's instructions (Promega). The absolute LUC/REN ratio was measured in a TriStar Multimode Reader LB 942 (Berthold Technologies).

Chromatin immunoprecipitation (ChIP) assay

The *OsPRMT6a* promoter and full-length sequence, spanning 6.8 kb, were amplified and

inserted into the *NcoI* restriction site upstream of LUC in the transient expression vector pGreenII 0800-LUC (Zhou et al., 2013) to generate the *pGreenII 0800-6A-LUC* reporter construct. The *pGreenII 0800-6A-LUC* and *p35S:OsMYC2-GFP* plasmids were cotransfected into young tobacco leaves. The solubilized chromatin was then immunoprecipitated using an anti-GFP antibody or rabbit immunoglobulin G (#2729, Cell Signaling Technology) at 4 °C for 8 hours. After immunoprecipitation, DNA was collected using Magna ChIP™ protein A magnetic beads (16-661, EMD Millipede Corporation). For each ChIP–qPCR, the DNA recovered from the immunoprecipitate was used as a template. The detailed methods have been previously described (Li et al., 2011).

Data availability

The raw RNA-seq data reported in this paper have been deposited the Genome Sequence Archive (Chen et al., 2021) in National Genomics Data Center (CNCB-NGDC members and partners, 2022), China National Center for Bioinformation / Beijing Institute of Genomics, Chinese Academy of Sciences (GSA: CRA016196) that are publicly accessible at https://ngdc.cncb.ac.cn/gsa, and in the National Center for Biotechnology Information (NCBI) Sequence Read Archive (SRA) under accession number PRJNA1034168.

References

Acosta, I.F., Laparra, H., Romero, S.P., Schmelz, E., Hamberg, M., Mottinger, J.P., Moreno, M.A., and Dellaporta, S.L. (2009). *tasselseed1* is a lipoxygenase affecting jasmonic acid signaling in sex determination of maize. Science **323**:262-265.

Ahmad, A., Dong, Y., and Cao, X. (2011). Characterization of the *PRMT* gene family in rice reveals conservation of arginine methylation. PLoS One **6**:e22664.

Bedford, M.T., and Clarke, S.G. (2009). Protein arginine methylation in mammals: who, what, and why. Mol. Cell **33**:1-13.

Blanc, R.S., and Richard, S. (2017). Arginine methylation: the coming of age. Mol. Cell **65**:8-24.

Blifernez, O., Wobbe, L., Niehaus, K., and Kruse, O. (2011). Protein arginine methylation modulates light-harvesting antenna translation in *Chlamydomonas reinhardtii*. Plant J. **65**:119-130.

Brown, R.L., Kazan, K., McGrath, K.C., Maclean, D.J., and Manners, J.M. (2003). A role for the GCC-box in jasmonate-mediated activation of the *PDF1.2* gene of Arabidopsis. Plant Physiol. **132**:1020-1032.

Browse, J., and Howe, G.A. (2008). New weapons and a rapid response against insect attack. Plant Physiol. **146**:832-838.

Cai, Q., Yuan, Z., Chen, M., Yin, C., Luo, Z., Zhao, X., Liang, W., Hu, J., and Zhang, D. (2014). Jasmonic acid regulates spikelet development in rice. Nat. Commun. **5**:3476.

Cao, L., Tian, J., Liu, Y., Chen, X., Li, S., Persson, S., Lu, D., Chen, M., Luo, Z., Zhang, D., et al. (2021). Ectopic expression of OsJAZ6, which interacts with OsJAZ1, alters JA signaling and spikelet development in rice. Plant J. **108**:1083-1096.

Carr, S.M., Munro, S., Kessler, B., Oppermann, U., and La Thangue, N.B. (2011). Interplay between lysine methylation and Cdk phosphorylation in growth control by the retinoblastoma protein. Embo J. **30**:317-327.

Chen, T., Chen, X., Zhang, S., Zhu, J., Tang, B., Wang, A., Dong, L., Zhang, Z., Yu, C., Sun, Y., et al. (2021). The Genome Sequence Archive family: toward explosive data growth and diverse data types. Genom. Proteom. Bioinf. **19**:578-583.

Chen, Z.X., Wu, J.G., Ding, W.N., Chen, H.M., Wu, P., and Shi, C.H. (2006). Morphogenesis and molecular basis on naked seed rice, a novel homeotic mutation of *OsMADS1* regulating transcript level of *AP3* homologue in rice. Planta **223**:882-890.

Cheng, X., Collins, R.E., and Zhang, X. (2005). Structural and sequence motifs of protein (histone) methylation enzymes. Annu. Rev. Biophys. Biomol. Struct. **34**:267-294.

Cheong, Y.H., Chang, H.S., Gupta, R., Wang, X., Zhu, T., and Luan, S. (2002). Transcriptional profiling reveals novel interactions between wounding, pathogen, abiotic stress, and hormonal responses in Arabidopsis. Plant Physiol. **129**:661-677.

Chico, J.M., Lechner, E., Fernandez-Barbero, G., Canibano, E., Garcia-Casado, G., Franco-Zorrilla, J.M., Hammann, P., Zamarreno, A.M., Garcia-Mina, J.M., Rubio, V., et al. (2020). $CUL3^{BPM}$ E3 ubiquitin ligases regulate MYC2, MYC3, and MYC4 stability and JA responses. Proc. Natl. Acad. Sci. U. S. A. **117**:6205-6215.

Chini, A., Fonseca, S., Fernandez, G., Adie, B., Chico, J.M., Lorenzo, O., Garcia-Casado, G., Lopez-Vidriero, I., Lozano, F.M., Ponce, M.R., et al. (2007). The JAZ family of repressors is the missing link in jasmonate signalling. Nature **448**:666-671.

Chung, H.S., and Howe, G.A. (2009). A critical role for the TIFY motif in repression of jasmonate signaling by a stabilized splice variant of the JASMONATE ZIM-domain protein JAZ10 in Arabidopsis. Plant Cell **21**:131-145.

Cui, R., Han, J., Zhao, S., Su, K., Wu, F., Du, X., Xu, Q., Chong, K., Theissen, G., and Meng, Z. (2010). Functional conservation and diversification of class E floral homeotic genes in rice (*Oryza sativa*). Plant J. **61**:767-781.

Devoto, A., Nieto-Rostro, M., Xie, D., Ellis, C., Harmston, R., Patrick, E., Davis, J., Sherratt, L., Coleman, M., and Turner,

J.G. (2002). COI1 links jasmonate signalling and fertility to the SCF ubiquitin-ligase complex in Arabidopsis. Plant J. **32**:457-466.

Dombrecht, B., Xue, G.P., Sprague, S.J., Kirkegaard, J.A., Ross, J.J., Reid, J.B., Fitt, G.P., Sewelam, N., Schenk, P.M., Manners, J.M., et al. (2007). MYC2 differentially modulates diverse jasmonate-dependent functions in Arabidopsis. Plant Cell **19**:2225-2245.

Duan, E., Wang, Y., Li, X., Lin, Q., Zhang, T., Wang, Y., Zhou, C., Zhang, H., Jiang, L., Wang, J., et al. (2019). OsSHI1 regulates plant architecture through modulating the transcriptional activity of IPA1 in rice. Plant Cell **31**:1026-1042.

Estève, P.O., Chang, Y., Samaranayake, M., Upadhyay, A.K., Horton, J.R., Feehery, G.R., Cheng, X., and Pradhan, S. (2011). A methylation and phosphorylation switch between an adjacent lysine and serine determines human DNMT1 stability. Nat. Struct. Mol. Biol. **18**:42-48.

Fang, L., Zhang, L., Wei, W., Jin, X., Wang, P., Tong, Y., Li, J., Du, J.X., and Wong, J. (2014). A methylation-phosphorylation switch determines Sox2 stability and function in ESC maintenance or differentiation. Mol. Cell **55**:537-551.

Feng, X., Zhang, L., Wei, X., Zhou, Y., Dai, Y., and Zhu, Z. (2020). OsJAZ13 negatively regulates jasmonate signaling and activates hypersensitive cell death response in rice. Int. J. Mol. Sci. **21**.

Goossens, J., Mertens, J., and Goossens, A. (2017). Role and functioning of bHLH transcription factors in jasmonate signalling. J. Exp. Bot. **68**:1333-1347.

Guo, Q., Yoshida, Y., Major, I.T., Wang, K., Sugimoto, K., Kapali, G., Havko, N.E., Benning, C., and Howe, G.A. (2018). JAZ repressors of metabolic defense promote growth and reproductive fitness in Arabidopsis. Proc. Natl. Acad. Sci. U. S. A. **115**:E10768-E10777.

Hang, R., Liu, C., Ahmad, A., Zhang, Y., Lu, F., and Cao, X. (2014). Arabidopsis protein arginine methyltransferase 3 is required for ribosome biogenesis by affecting precursor ribosomal RNA processing. Proc. Natl. Acad. Sci. U. S. A. **111**:16190-16195.

He, Y., Hong, G., Zhang, H., Tan, X., Li, L., Kong, Y., Sang, T., Xie, K., Wei, J., Li, J., et al. (2020). The OsGSK2 kinase integrates brassinosteroid and jasmonic acid signaling by interacting with OsJAZ4. Plant Cell **32**:2806-2822.

Hiei, Y., Ohta, S., Komari, T., and Kumashiro, T. (1994). Efficient transformation of rice (*Oryza sativa L.*) mediated by *Agrobacterium* and sequence analysis of the boundaries of the T-DNA. Plant J. **6**:271-282.

Hong, S., Song, H.R., Lutz, K., Kerstetter, R.A., Michael, T.P., and McClung, C.R. (2010). Type II protein arginine methyltransferase 5 (PRMT5) is required for circadian period determination in *Arabidopsis thaliana*. Proc. Natl. Acad. Sci. U. S. A. **107**:21211-21216.

Hori, Y., Kurotani, K., Toda, Y., Hattori, T., and Takeda, S. (2014). Overexpression of the JAZ factors with mutated jas domains causes pleiotropic defects in rice spikelet development. Plant Signal Behav. **9**:e970414.

Hu, S., Yu, K., Yan, J., Shan, X., and Xie, D. (2023). Jasmonate perception: Ligand-receptor interaction, regulation, and evolution. Mol. Plant **16**:23-42.

Huang, H., Liu, B., Liu, L., and Song, S. (2017). Jasmonate action in plant growth and development. J. Exp. Bot. **68**:1349-1359.

Ikeda, K., Sunohara, H., and Nagato, Y. (2004). Developmental course of inflorescence and spikelet in rice. Breed. Sci. **54**:147–156.

Ivanov, G.S., Ivanova, T., Kurash, J., Ivanov, A., Chuikov, S., Gizatullin, F., Herrera-Medina, E.M., Rauscher, F., 3rd,

Reinberg, D., and Barlev, N.A. (2007). Methylation-acetylation interplay activates p53 in response to DNA damage. Mol. Cell. Biol. **27**:6756-6769.

Jeon, J.S., Jang, S., Lee, S., Nam, J., Kim, C., Lee, S.H., Chung, Y.Y., Kim, S.R., Lee, Y.H., Cho, Y.G., et al. (2000). *leafy hull sterile1* is a homeotic mutation in a rice MADS box gene affecting rice flower development. Plant Cell **12**:871-884.

Katsir, L., Schilmiller, A.L., Staswick, P.E., He, S.Y., and Howe, G.A. (2008). COI1 is a critical component of a receptor for jasmonate and the bacterial virulence factor coronatine. Proc. Natl. Acad. Sci. U. S. A. **105**:7100-7105.

Kim, E.H., Kim, Y.S., Park, S.H., Koo, Y.J., Choi, Y.D., Chung, Y.Y., Lee, I.J., and Kim, J.K. (2009). Methyl jasmonate reduces grain yield by mediating stress signals to alter spikelet development in rice. Plant Physiol. **149**:1751-1760.

Komatsu, M., Chujo, A., Nagato, Y., Shimamoto, K., and Kyozuka, J. (2003). *FRIZZY PANICLE* is required to prevent the formation of axillary meristems and to establish floral meristem identity in rice spikelets. Development **130**:3841-3850.

Lee, D.Y., and An, G. (2012). Two AP2 family genes, *supernumerary bract* (*SNB*) and *Osindeterminate spikelet 1* (*OsIDS1*), synergistically control inflorescence architecture and floral meristem establishment in rice. Plant J. **69**:445-461.

Lee, D.Y., Lee, J., Moon, S., Park, S.Y., and An, G. (2007). The rice heterochronic gene *SUPERNUMERARY BRACT* regulates the transition from spikelet meristem to floral meristem. Plant J. **49**:64-78.

Lee, H.Y., Seo, J.S., Cho, J.H., Jung, H., Kim, J.K., Lee, J.S., Rhee, S., and Do Choi, Y. (2013). *Oryza sativa COI* homologues restore jasmonate signal transduction in Arabidopsis *coi1-1* mutants. PLoS One **8**:e52802.

Lei, Y., Lu, L., Liu, H.Y., Li, S., Xing, F., and Chen, L.L. (2014). CRISPR-P: a web tool for synthetic single-guide RNA design of CRISPR-system in plants. Mol. Plant **7**:1494-1496.

Lescot, M., Dehais, P., Thijs, G., Marchal, K., Moreau, Y., Van de Peer, Y., Rouze, P., and Rombauts, S. (2002). PlantCARE, a database of plant cis-acting regulatory elements and a portal to tools for *in silico* analysis of promoter sequences. Nucleic Acids Res. **30**:325-327.

Li, H., Xue, D., Gao, Z., Yan, M., Xu, W., Xing, Z., Huang, D., Qian, Q., and Xue, Y. (2009). A putative lipase gene *EXTRA GLUME1* regulates both empty-glume fate and spikelet development in rice. Plant J. **57**:593-605.

Li, H., Liang, W., Hu, Y., Zhu, L., Yin, C., Xu, J., Dreni, L., Kater, M.M., and Zhang, D. (2011). Rice *MADS6* interacts with the floral homeotic genes *SUPERWOMAN1*, *MADS3*, *MADS58*, *MADS13*, and *DROOPING LEAF* in specifying floral organ identities and meristem fate. Plant Cell **23**:2536-2552.

Lim, J., Moon, Y.H., An, G., and Jang, S.K. (2000). Two rice MADS domain proteins interact with *OsMADS1*. Plant Mol. Biol. **44**:513-527.

Lin, Q., Wang, D., Dong, H., Gu, S., Cheng, Z., Gong, J., Qin, R., Jiang, L., Li, G., Wang, J.L., et al. (2012). Rice APC/C^{TE} controls tillering by mediating the degradation of MONOCULM 1. Nat. Commun. **3**:752.

Lorenzo, O., Chico, J.M., Sánchez-Serrano, J.J., and Solano, R. (2004). *JASMONATE-INSENSITIVE1* encodes a MYC transcription factor essential to discriminate between different jasmonate-regulated defense responses in Arabidopsis. Plant Cell **16**:1938-1950.

Lucher, L.A., and Lego, T. (1989). Use of the water-soluble fluor sodium salicylate for fluorographic detection of tritium in thin-layer chromatograms and nitrocellulose blots. Anal. Biochem. **178**:327-330.

Malcomber, S.T., and Kellogg, E.A. (2004). Heterogeneous expression patterns and separate roles of the *SEPALLATA* gene *LEAFY HULL STERILE1* in grasses. Plant Cell **16**:1692-1706.

Mou, Z., He, Y., Dai, Y., Liu, X., and Li, J. (2000). Deficiency in fatty acid synthase leads to premature cell death and dramatic

alterations in plant morphology. Plant Cell **12**:405-418.

partners, C.-N.m.a. (2022). Database resources of the National Genomics Data Center, China National Center for Bioinformation in 2022. Nucleic Acids Res. **50**:D27-d38.

Pauwels, L., Morreel, K., De Witte, E., Lammertyn, F., Van Montagu, M., Boerjan, W., Inzé, D., and Goossens, A. (2008). Mapping methyl jasmonate-mediated transcriptional reprogramming of metabolism and cell cycle progression in cultured Arabidopsis cells. Proc. Natl. Acad. Sci. U. S. A. **105**:1380-1385.

Pei, Y., Niu, L., Lu, F., Liu, C., Zhai, J., Kong, X., and Cao, X. (2007). Mutations in the Type II protein arginine methyltransferase AtPRMT5 result in pleiotropic developmental defects in Arabidopsis. Plant Physiol. **144**:1913-1923.

Ren, D., Li, Y., Zhao, F., Sang, X., Shi, J., Wang, N., Guo, S., Ling, Y., Zhang, C., Yang, Z., et al. (2013). MULTI-FLORET SPIKELET1, which encodes an AP2/ERF protein, determines spikelet meristem fate and sterile lemma identity in rice. Plant Physiol. **162**:872-884.

Reymond, P., Weber, H., Damond, M., and Farmer, E.E. (2000). Differential gene expression in response to mechanical wounding and insect feeding in Arabidopsis. Plant Cell **12**:707-720.

Scebba, F., De Bastiani, M., Bernacchia, G., Andreucci, A., Galli, A., and Pitto, L. (2007). PRMT11: a new Arabidopsis MBD7 protein partner with arginine methyltransferase activity. Plant J. **52**:210-222.

Schmitz, R.J., Sung, S., and Amasino, R.M. (2008). Histone arginine methylation is required for vernalization-induced epigenetic silencing of *FLC* in winter-annual *Arabidopsis thaliana*. Proc. Natl. Acad. Sci. U. S. A. **105**:411-416.

Sheard, L.B., Tan, X., Mao, H., Withers, J., Ben-Nissan, G., Hinds, T.R., Kobayashi, Y., Hsu, F.F., Sharon, M., Browse, J., et al. (2010). Jasmonate perception by inositol-phosphate-potentiated COI1-JAZ co-receptor. Nature **468**:400-405.

Taylor, S.C., Berkelman, T., Yadav, G., and Hammond, M. (2013). A defined methodology for reliable quantification of Western blot data. Mol. Biol. **55**:217-226.

Thines, B., Parlan, E.V., and Fulton, E.C. (2019). Circadian network interactions with jasmonate signaling and defense. Plants-Basel **8**.

Thines, B., Katsir, L., Melotto, M., Niu, Y., Mandaokar, A., Liu, G., Nomura, K., He, S.Y., Howe, G.A., and Browse, J. (2007). JAZ repressor proteins are targets of the SCF^{COI1} complex during jasmonate signalling. Nature **448**:661-665.

Tong, H., Jin, Y., Liu, W., Li, F., Fang, J., Yin, Y., Qian, Q., Zhu, L., and Chu, C. (2009). DWARF AND LOW-TILLERING, a new member of the GRAS family, plays positive roles in brassinosteroid signaling in rice. Plant J. **58**:803-816.

Waadt, R., and Kudla, J. (2008). In planta visualization of protein interactions using bimolecular fluorescence complementation (BiFC). CSH Protoc. **2008**:pdb prot4995.

Wang, F., Zhu, D., Huang, X., Li, S., Gong, Y., Yao, Q., Fu, X., Fan, L.M., and Deng, X.W. (2009). Biochemical insights on degradation of Arabidopsis DELLA proteins gained from a cell-free assay system. Plant Cell **21**:2378-2390.

Wang, X., Zhang, Y., Ma, Q., Zhang, Z., Xue, Y., Bao, S., and Chong, K. (2007). SKB1-mediated symmetric dimethylation of histone H4R3 controls flowering time in Arabidopsis. Embo J. **26**:1934-1941.

Wolf, S.S. (2009). The protein arginine methyltransferase family: an update about function, new perspectives and the physiological role in humans. Cell. Mol. Life Sci. **66**:2109-2121.

Wolters, H., and Jurgens, G. (2009). Survival of the flexible: hormonal growth control and adaptation in plant development. Nat. Rev. Genet. **10**:305-317.

Wu, H., Ye, H., Yao, R., Zhang, T., and Xiong, L. (2015). OsJAZ9 acts as a transcriptional regulator in jasmonate signaling and

modulates salt stress tolerance in rice. Plant Sci. **232**:1-12.

Wu, Y., Wang, Y., Mi, X.F., Shan, J.X., Li, X.M., Xu, J.L., and Lin, H.X. (2016). The QTL *GNP1* encodes GA20ox1, which increases grain number and yield by increasing cytokinin activity in rice panicle meristems. PLoS Genet. **12**:e1006386.

Xu, L., Liu, F., Lechner, E., Genschik, P., Crosby, W.L., Ma, H., Peng, W., Huang, D., and Xie, D. (2002). The SCF^{COI1} ubiquitin-ligase complexes are required for jasmonate response in Arabidopsis. Plant Cell **14**:1919-1935.

Yamada, S., Kano, A., Tamaoki, D., Miyamoto, A., Shishido, H., Miyoshi, S., Taniguchi, S., Akimitsu, K., and Gomi, K. (2012). Involvement of OsJAZ8 in jasmonate-induced resistance to bacterial blight in rice. Plant Cell Physiol. **53**:2060-2072.

Yamagata, K., Daitoku, H., Takahashi, Y., Namiki, K., Hisatake, K., Kako, K., Mukai, H., Kasuya, Y., and Fukamizu, A. (2008). Arginine methylation of FOXO transcription factors inhibits their phosphorylation by Akt. Mol. Cell **32**:221-231.

Yan, D., Zhang, Y., Niu, L., Yuan, Y., and Cao, X. (2007). Identification and characterization of two closely related histone H4 arginine 3 methyltransferases in *Arabidopsis thaliana*. Biochem. J. **408**:113-121.

Yan, H., Yoo, M.J., Koh, J., Liu, L., Chen, Y., Acikgoz, D., Wang, Q., and Chen, S. (2014). Molecular reprogramming of Arabidopsis in response to perturbation of jasmonate signaling. J. Proteome Res. **13**:5751-5766.

Yang, D.-L., Yao, J., Mei, C.-S., Tong, X.-H., Zeng, L.-J., Li, Q., Xiao, L.-T., Sun, T.-p., Li, J., Deng, X.-W., et al. (2012). Plant hormone jasmonate prioritizes defense over growth by interfering with gibberellin signaling cascade. Proc. Natl. Acad. Sci. U. S. A. **109**:E1192-1200.

Yang, J., Huang, J., Dasgupta, M., Sears, N., Miyagi, M., Wang, B., Chance, M.R., Chen, X., Du, Y., Wang, Y., et al. (2010). Reversible methylation of promoter-bound STAT3 by histone-modifying enzymes. Proc. Natl. Acad. Sci. U. S. A. **107**:21499-21504.

Ye, H., Du, H., Tang, N., Li, X., and Xiong, L. (2009). Identification and expression profiling analysis of *TIFY* family genes involved in stress and phytohormone responses in rice. Plant Mol. Biol. **71**:291-305.

Yoshida, A., Suzaki, T., Tanaka, W., and Hirano, H.Y. (2009a). The homeotic gene *long sterile lemma* (*G1*) specifies sterile lemma identity in the rice spikelet. Proc. Natl. Acad. Sci. U. S. A. **106**:20103-20108.

Yoshida, H., and Nagato, Y. (2011). Flower development in rice. J. Exp. Bot. **62**:4719-4730.

Yoshida, Y., Sano, R., Wada, T., Takabayashi, J., and Okada, K. (2009b). Jasmonic acid control of GLABRA3 links inducible defense and trichome patterning in Arabidopsis. Development **136**:1039-1048.

You, X., Zhu, S., Zhang, W., Zhang, J., Wang, C., Jing, R., Chen, W., Wu, H., Cai, Y., Feng, Z., et al. (2019). OsPEX5 regulates rice spikelet development through modulating jasmonic acid biosynthesis. New Phytol. **224**:712-724.

Zhang, T., Li, Y., Ma, L., Sang, X., Ling, Y., Wang, Y., Yu, P., Zhuang, H., Huang, J., Wang, N., et al. (2017). *LATERAL FLORET 1* induced the three-florets spikelet in rice. Proc. Natl. Acad. Sci. U. S. A. **114**:9984-9989.

Zhang, Z., Zhang, S., Zhang, Y., Wang, X., Li, D., Li, Q., Yue, M., Li, Q., Zhang, Y.E., Xu, Y., et al. (2011). Arabidopsis floral initiator SKB1 confers high salt tolerance by regulating transcription and pre-mRNA splicing through altering histone H4R3 and small nuclear ribonucleoprotein LSM4 methylation. Plant Cell **23**:396-411.

Zhou, F., Lin, Q., Zhu, L., Ren, Y., Zhou, K., Shabek, N., Wu, F., Mao, H., Dong, W., Gan, L., et al. (2013). D14-SCF^{D3}-dependent degradation of D53 regulates strigolactone signalling. Nature **504**:406-410.

Author contributions

Jianmin Wan, Qibing Lin and Zhijun Cheng supervised the project; Kun Dong designed the research; Kun Dong, Qibing Lin and Chuanyin Wu wrote the paper; Fuqing Wu provided the plant material; Kun Dong performed most of the experiments; Kun Dong and Siqi Cheng analyzed the data; Siqi Cheng performed the cytological observations; Shuai Li performed the yeast one-hybrid assay, LUC transient reporter gene assay and ChIP assay; Miao Feng performed the RNA *in situ* hybridization; Rong Miao performed the subcellular localization assay; Chuanyin Wu, Qibing Lin, Fuqing Wu, Feng Zhang, Xiaoman You, Xin Zhang, Cailin Lei, Yulong Ren and Shanshan Zhu provided technical assistance; Siqi Cheng, Xin Jin, Xinxin Xing, and Yanqi Chang performed a portion of the RT−qPCR analysis; Xiuping Guo generated the transgenic plants; and Kun Dong, Siqi Cheng, Peiran Wang and Shuang Zhang cultivated the transgenic plants in the field.

Acknowledgments

We thank Prof. Qiang Cai (College of Life Sciences, Wuhan University) and Prof. Zheng Yuan (School of Life Sciences and Biotechnology, Shanghai Jiao Tong University) for providing morphology data of the *eg1-1* and *eg2-1D* mutants. This work was supported by grants from the National Key R&D Program of China (2022YFD1200100) and the National Natural Science Foundation of China (No. 92035301 and No. 31771765).

Declaration of interests

The authors declare no competing interests.

Figure Legends

Figure 1. Abnormal spikelet morphologies of *osprmt6a-1* mutant.

A, Targeted mutation to *OsPRMT6a* by CRISPR/Cas9 technology. The diagram shows the genomic structure of *OsPRMT6a*. Arrows indicate target sites. Exons, Introns and Untranslated regions (UTR) are denoted by black boxes, lines and white boxes, respectively. The right panel displays sequence alignment of WT, *osprmt6a-1* and *osprmt6a-2,* highlighting the CRISPR/Cas9-induced mutated sites. Blue font, showing 18 bp CRISPR/Cas9 target sequences adjacent to the underlined protospacer adjacent motifs (PAMs). **B**-**H**, Spikelet morphologies, including normal spikelets in WT (**B**), and various spikelet morphologies in *osprmt6a-1*, consisting of normal spikelet (**C**), and abnormal spikelets with long sterile lemma (**D**), long sterile lemma & spikelet-like (**E**), long sterile lemma & lemma-like (**F**), two long sterile lemmas & spikelet-like (**G**), and one separate long sterile lemma and one sterile lemma (**H**). The ratio of specific mutation type (2020, Shunyi district, Beijing) is marked in the lower left corner. **I**-**O**, Transverse resin semi-thin sections from **B**-**H**. **P**, WT floret with six stamens, two lodicules, one carpel and two stigmas. The lemma and palea were removed for observation. **Q**-**U**, *osprmt6a-1* produces normal florets like WT (**Q**) and abnormal florets with eight stamens (**R**), three stigmas & stamen-like organ (**S**), severely malformed carpel, stamen, and stigma (**T**), and a degenerated spikelet (**U**). le, lemma; lel, lemma-like; pa, palea; sl, sterile lemma; st, stamen; lo, lodicule; fi, filament; stg, stigma; stgl, stigma-like; lsl, long sterile lemma; spl, spikelet-like; ca, carpel; cal, carpel-like; stl, stamen-like. Scale bars, 2 mm (**B**-**H**), 500 μM (**I**-**O**), 1 mm (**P**-**U**).

Figure 2. OsPRMT6a physically interacts with OsJAZ1 to methylate arginine residues of OsJAZ1.

A, *In vivo* Co-Immunoprecipitation (CoIP) assay showing the interaction between OsPRMT6a

and OsJAZ1 in *N. benthamiana* leaves. The molecular weight (MW) of OsJAZ1 and GFP is 23.02 kDa and 27.12 kDa. The theoretical MW of the OsJAZ1-GFP fusion protein, including the linking residue, is 51.28 kDa. Due to post-translational modifications such as arginine methylation and ubiquitination, the observed band for OsJAZ1-GFP appears slightly higher than the 55 kDa band of the molecular weight marker. **B**, *In vitro* pull-down assay showing the interaction of OsPRMT6a with OsJAZ1. His-OsPRMT6a proteins were incubated with the MBP-OsJAZ1 or MBP proteins. Protein samples were immunoprecipitated with anti-His antibodies and immunoblotted with anti-His and anti-MBP antibodies. **C**, Luciferase complementation imaging (LCI) assay showing the interaction of OsPRMT6a with OsJAZ1 in *N. benthamiana* leaves. The pseudocolor bar (right panel) shows the range of luminescence intensity in each image. **D**, Bimolecular fluorescence complementation (BiFC) assay showing the interaction between OsPRMT6a and OsJAZ1 in the leaf epidermal cells of *N. benthamiana*. **E**, OsPRMT6a methylated arginine residues of OsJAZ1 *in vitro*. Top and bottom panels, Western blots; middle panel, Coomassie brilliant blue staining. OsJAZ1 (WT/1K/5K) represent the wild-type OsJAZ1, OsJAZ1 with one arginine replaced by lysine and OsJAZ1 with five arginines replaced by lysine, respectively. **F**, OsPRMT6a methylated arginine residues of OsJAZ1 *in vivo*. α-HSP82 shows an equal amount of total proteins, α-OsJAZ1 shows an equal amount of OsJAZ1-GFP protein in the total proteins, and α-R (Arginine)-Methyl shows the levels of methylated arginine residues in OsJAZ1-GFP proteins in plants. **G**, OsJAZ1 protein sequence showing methylated arginine residues (marked with red font) *in vitro* by mass spectrometry analysis. The blue underlined residues represent the coverage extent of identified protein peptides. **H**, A table listing methylated peptides and their methylation modification status detected by mass spectrometry. **I**, A representative mass spectrometry result illustrating a methylated arginine residue in the GGEVEEEVAR peptide of OsJAZ1 protein. Scale bars, 20 μm. The symbols ‘‘-’’ and ‘‘+’’ denote the absence and presence of the corresponding proteins.

Figure 3. JAs promotes OsJAZ1 degradation in presence of OsPRMT6a.

A, **B**, Western blot analysis reveals that 2 mM MeJA induces the OsJAZ1 degradation in WT but not in *osprmt6a-1*, or the OsJAZ1-GFP degradation in *p35S:OsJAZ1-GFP/*WT but not in *p35S:OsJAZ1-GFP/osprmt6a-1* transgenic plants. **C**, Levels of JA and its amino acid derivative JA-Ile in seedlings and spikelets of WT and *osprmt6a-1*. **D**, Expression levels of *OsJAZ1* in 2-week-old seedlings or spikelets of WT, *osprmt6a-1*, *p35S:OsJAZ1-GFP*/WT and *p35S:OsJAZ1-GFP/osprmt6a-1* transgenic plants. **E**, Protein levels of OsJAZ1 in spikelets of WT and *osprmt6a-1* plants, or OsJAZ1-GFP in spikelets of *p35S:OsJAZ1-GFP*/WT and *p35S:OsJAZ1-GFP/osprmt6a-1* transgenic plants. **F**, *In vivo* dual-LUC-degradation assay using luciferase reporters, OsJAZ1-LUC and OsJAZ1 (5K)-LUC, transiently expressed in *N. benthamiana* leaves for 48 and 72 hours, respectively. Values = means ± s.e.m. (*n* = 3 replicates). Asterisks, statistically significant differences between samples (*P < 0.05, **P < 0.01 by the Student's t-test). **G**, Schematic representation of the OsJAZ1-LUC and OsJAZ1 (5K)-LUC constructs for the dual-LUC-degradation assay in (**C**). 35S, CaMV35S promoter; REN, Renilla luciferase; OsJAZ1(WT/5K)-LUC, fusion protein of OsJAZ1 (or OsJAZ1 (5K)) and Firefly luciferase. **H**, Cell-free degradation assay shows that MBP-OsJAZ1 is more easily degraded than MBP-OsJAZ1 (5K), and the proteasome inhibitor MG132 inhibits the degradation of MBP-OsJAZ1. Numbers below Western blot images represent the band density ratio of α-OsJAZ1/α-HSP82 (**A**, **B**, **E**), quantified using ImageJ.

Figure 4. OsPRMT6A promotes the interaction of OsJAZ1 with OsCOI1a or OsCOI1b, and thus its ubiquitination.

A, Y2H assay showing the interaction of OsCOI1b with OsJAZ1 in the presence of COR of different concentrations, no interaction of OsCOI1b with OsJAZ1 in the absence of COR, and no interaction of OsJAZ1 with OsCOI1a in the presence or absence of COR. BD, binding domain; AD, activating domain; the gradients indicate tenfold serial dilutions. **B,** *In vivo* CoIP showing the

interaction between OsCOI1a and OsJAZ1-GFP in WT and *osprmt6a-1* background. OsJAZ1-GFP in WT or *osprmt6a-1* were used as bait to immunoprecipitate the native OsCOI1a. **C**, Semi-*in vivo* CoIP showing the interaction between MBP-OsCOI1b and OsJAZ1-GFP in WT and *osprmt6a-1* background. OsJAZ1-GFP in WT or *osprmt6a-1* were employed as bait to immunoprecipitate the exogenously added prokaryotic-expressed MBP-OsCOI1b. **D, E**, *In vivo* CoIP showing the stronger interaction of OsCOI1a-Flag or OsCOI1b-Flag with OsJAZ1-GFP than with OsJAZ1 (5K)-GFP in rice protoplasts. OsJAZ1-GFP or OsJAZ1-GFP (5K) were used as bait to immunoprecipitate the OsCOI1a-Flag or OsCOI1b-Flag. **F**, LCI assay shows that the interaction between OsPRMT6a and OsJAZ1 depends on OsPRMT6a in *N. benthamiana* leaves. The pseudocolor bar (right panel) shows the range of luminescence intensity in each image. **G**, BiFC assay shows that the interaction between OsPRMT6a and OsJAZ1 depends on OsPRMT6a in the leaf epidermal cells of *N. benthamiana.* **H**, *In vitro* ubiquitination assay showing that OsJAZ1 is more ubiquitinated by WT than by *osprmt6a-1* plant extracts, while OsJAZ1 (5K) exhibits weak ubiquitination by WT plant extracts. Scale bars, 50 μm. The symbols ‘‘-’’ and ‘‘+’’ denote the absence and presence of the corresponding proteins.

Figure 5. The arginine demethylation status of OsJAZ1 impedes JA responses and normal spikelet development.

A, Expression changes of JA signaling pathway genes. The horizontal axis of the line chart is the sampling time of 25-day-old seedlings after 2 mM MeJA treatment. **B**, RNA-seq analysis of WT vs *osprmt6a-1* DEG enriched KEGG pathway scatter plot. **C**, RT-qPCR results validate the clustering results of RNA-seq about JA signaling pathway. Values are presented as means ± s.e.m. (n = 3 replicates). Asterisks represent statistically significant differences in the relative expression of corresponding genes genes between WT and *osprmt6a-1* at the same time point and “N.S.” denotes no significant (*P < 0.05, **P < 0.01 by the Student’s t-test). **D**-**J**, Spikelet morphologies, including normal spikelets in WT (**D**), and various spikelet morphologies like

normal spikelet (**E**), abnormal spikelets with long sterile lemma (**F**), two long sterile lemmas (**G**), a long sterile lemma & a spikelet-like structure (**H**), two separate long sterile lemmas (**I**) and one separate long sterile lemma (**J**) in *p35S: OsJAZ1 (5K)-GFP*/WT transgenic plants. The ratio of specific mutation type is marked in the lower left corner. **K**, WT floret with six stamens, two lodicules, one carpel and two stigmas. The lemma and palea were removed for observation. **L**-**P**, *p35S: OsJAZ1 (5K)-GFP*/WT transgenic plants with normal floret like WT (**L**), and abnormal florets with seven stamens (**M**), long sterile lemma & lodicule-like (**N**), three stamens & stigma-like (**O**) or spikelet-like (**P**). Scale bars, 2 mm (**D**-**J**), 1 mm (**K**-**P**). le, lemma; pa, palea; st, stamen; stl stamen-like; sl, sterile lemma; lo, lodicule; stg, stigma; stgl, stigma-like; lsl, long sterile lemma; spl, spikelet-like; ca, carpel; cal, carpel-like; lol, lodicule-like.

Figure 6. MeJA represses the *OsPRMT6a* expression through OsMYC2.

A, mRNA level of *OsPRMT6a* decreases following 1 mM MeJA treatment in 12-day-old WT seedlings. **B**, Protein level of OsPRMT6a decreases following 1 mM MeJA treatment in 12-day-old *pUbi:OsPRMT6a-Flag* transgenic plants. Numbers below the images represent the band density ratio of α-Flag/α-HSP82 quantified by software ImageJ. **C**, Diagram of the *OsPRMT6a* genomic region featuring DNA fragments (red lines, P1 to P6) with the G-box (5'-CACGTG/CACATG-3') motif. White boxes, untranslated region; black boxes, exons; black lines, introns. **D**, ChIP-qPCR analysis indicating amplification of promoter fragments P2 and P3 from IP pulled down by the anti-GFP antibody. The control, immunoglobulin G was set as 1. **E**, Y1H assays of the binding regions of OsMYC2 in the promoter regions of *OsPRMT6a*. Series of promoter fragments of *OsPRMT6a* were fused to upstream region of LacZ reporter gene for OsMYC2 binding test. AD, the empty pB42AD, negative control. **F**, EMSA assay showing direct binding of OsMYC2 to the G-box motif in the *OsPRMT6a* promoter. The arrow indicates the shifted band representing the protein–DNA complex. The symbols ''-'' and ''+'' denote the absence and presence of the corresponding proteins or probes. **G**, Schematic representation of

the effector and reporter constructs. Full-length coding regions of OsMYC2-GFP fusion protein or GFP protein under control of the 35S promoter, as the effectors. The Firefly luciferase gene LUC driven by the *OsPRMT6a* promoters and the Renilla luciferase gene Ren driven by the 35S promoter, as the reporters. **H**, Transient dual-LUC reporter gene assays revealing OsMYC2 inhibition of *OsPRMT6a* transcription. **I**, mRNA level of *OsPRMT6a* in *loss-of-function* mutant *osmyc2* remain relatively unchanged under the treatment of 1 mM MeJA in 12-day-old seedlings. Values are means ± s.e.m. (n = 3 replicates). Asterisks indicate significant differences, and "N.S." denotes no significant (**P < 0.01 by the Student's t-test) in **A**, **D**, **H**, **I**.

Figure 7. Schematic model depicts that the arginine methylation of OsJAZ1 by OsPRMT6a promotes its degradation and thus JA signal transmit.

In WT, OsPRMT6a methylates arginines of OsJAZ1. The arginine methylation of OsJAZ1 enhances its interaction with OsCOI1a/OsCOI1b, thus promoting the ubiquitination of OsJAZ1 by the $SCF^{OsCOI1a/OsCOI1b}$ complex, subsequently the degradation of OsJAZ1 by 26S proteasome. The degradation of OsJAZ1 frees OsMYC2 to activate (or repress) JA-responsive genes, including *OsPRMT6a*, ultimately promoting the transmission of the JA signal to maintain normal spikelet development. And the OsPRMT6a protein accumulates at normal temperatures but decreases at high temperatures, leading to dynamic changes in OsPRMT6a-regulated arginine methylation and protein level of OsJAZ1 with temperature fluctuations. SAM, methyl donor S-adenosylmethionine. M, methyl.

However, in *loss-of-function osprmt6a* mutants, the dynamic changes of OsPRMT6a-regulated arginine methylation and protein level of OsJAZ1 are not observed, leading to the constant stabilization of OsJAZ1. This stabilization hinders JA signaling transduction, ultimately causing abnormal spikelet development.

Supplementary Figure 1. Scanning electron micrographs of WT and *osprmt6a-1* spikelets at stages Sp5 to Sp6.

A, WT spikelet display six stamen primordia and a normal floral meristem. **B**-**F**, *osprmt6a-1* mutant exhibit varied spikelet morphologies, including normal spikelet (**B**), bulged floral meristem (**C**), abnormal long sterile lemma & ectopic stamen-like (**D**), abnormal cylindrical glume-like (**E**), and ectopic stamen-like (**F**). le, lemma; lel, lemma-like; pa, palea; fm, floral meristem; st, stamen; estl, ectopic stamen-like; sl, sterile lemma; lsl, long sterile lemma; cgl, cylindrical glume-like. Scale bars, 100 μm (**A**-**F**).

Supplementary Figure 2. Phenotypic analyses of *osprmt6a* mutants.

A, Plant phenotype of WT and two *osprmt6a* mutants (*osprmt6a-1* and *osprmt6a-2*) at heading stage. **B**, **C**, Panicle phenotype (**B**) and pollen iodine staining (**C**) of WT and two *osprmt6a* mutants. **D**-**I**, Difference in plant height and internode length (**D**), tiller number (**E**), seed setting rate (**F**), branch number (**G**), grain number per panicle (**H**) and grain size (**I**) between WT and two *osprmt6a* mutants.

Scale bars, 15 cm (**A**), 3 cm (**B**), 2 mm (**C**). Values are means ± s.d. (**D, E,** n = 30 plants; **F**, **G**, **H**, n = 30 panicles; **I**, n = 30 seeds) and asterisks represent statistically significant differences between the samples (*P < 0.05, **P < 0.01 by the Student's t-test). The whole plant (**A**) and the anthers (**C**) were sampled in the field, and the panicles (**B**) were sampled in the greenhouse. PBN, primary branches number; SBN, secondary branches number; GNP, grain number per panicle; FGN, filled grain number per panicle.

Supplementary Figure 3. Complement analyses of *OsPRMT6a*-RNAi lines and complement transgenic line.

A, Plant phenotype of *OsPRMT6a*-RNAi lines (Ri1 and Ri2) and complement transgenic line (C1). **B**, Expression levels of *OsPRMT6a* in line Ri1, Ri2 and C1. **C**, The typical spikelet of the WT exhibits a lemma, a palea, and two sterile lemmas; lines Ri1 and Ri2 exhibit abnormal spikelets similar to *osprmt6a-1*; line C1 exhibits normal spikelets similar to WT. **D**, Western blot analysis reveals that 2 mM MeJA induces OsJAZ1 degradation in line C1 but not in line Ri1. **E**, Expression levels of *OsJAZ1* in seedlings or spikelets of lines C1 and Ri1. Values are means ± s.e.m. (**B**, **E**, n = 3 replicates). Asterisks represent statistically significant differences between

samples (**P < 0.01 by the Student's t-test). **F**, Protein levels of OsJAZ1 in spikelets of line C1 and line Ri1 at heading stage. le, lemma; pa, palea; sl, sterile lemma; lsl, long sterile lemma; spl, spikelet-like. Scale bar, 15 cm (**A**), 2 mm (**C**).

Supplementary Figure 4. Phylogenetic tree of OsPRMT6a and its homologs in plant.

Using all the PRMTs from Arabidopsis and rice, as well as the OsPRMT6a orthologs found in 23 other species (with E-value less than $1e^{-180}$) from the NCBI database, we constructed a phylogenetic tree by neighbor-joining method. The bootstrap values represent the percentage of 1000 replicates, while the length of the branches is relative to the amino acid variation rates.

Supplementary Figure 5. Sequence alignment of OsPRMT6a with orthologs from other species.

The amino acids that are identical are highlighted with a black background while the similar ones are highlighted with a grey background. The motifs of the arginine methyltransferase, including I, post-I, post-II, post-III, Double E loop and THW loop, are enclosed in black boxes. The sequences used for the alignment include OsPRMT6a and OsPRMT6b from *Oryza Sativa*, AtPRMT6 from *Arabidopsis thaliana*, BRADI3g29470 from *Brachypodium distachyon*, SORBI3001G211900 from *Sorghum bicolor*, and GRMZM2G160752 from *Zea mays*.

Supplementary Figure 6. Transcriptional profiling of *OsPRMT6a* gene and subcellular localization of OsPRMT6a protein.

A, Expression pattern of *OsPRMT6a* in different tissues of Kitaake. Values are presented as means ± s.e.m. (n = 3 replicates). **B** and **C**, Subcellular localization of the OsPRMT6a–GFP fusion protein in rice protoplasts. D53–mCherry served as a nuclear marker (**B**) and SCAMP1-mCherry as a membrane marker (**C**). Free GFP was used as the control. **D**-**H**, mRNA *in situ* hybridization reveals that *OsPRMT6a* was predominantly expressed in the inflorescence meristem (IM) (**D**), primary branch meristem (PBM), bracts (BRC) (**E**), secondary branch meristem (SBM) (**F**), and spikelets (SP) (**G**) as indicated by arrowheads. **H**, The sense probe of *OsPRMT6a* was used as a negative control. Scale bars, 10 μm (**B**, **C**), 100 μm (**D**-**H**).

Supplementary Figure 7. OsPRMT6a interacts with some OsJAZs in yeast.

Y2H assay showing the interactions between OsPRMT6a and OsJAZs. BD, binding domain; AD,

activating domain; the transformed yeast cells were plated on DDO (synthetic dropout /-Trp/-Leu) and QDO (synthetic dropout /-Trp/-Leu/-His/-Ade); the gradients indicate tenfold serial dilutions.

Supplementary Figure 8. OsPRMT6a interacts with OsJAZ7 and OsJAZ8.

A, *In vivo* CoIP assay showing the interaction between OsPRMT6a and OsJAZ7/8 in *N. benthamiana* leaves. The molecular weight (MW) of OsJAZ7, OsJAZ8 and GFP is 25.54 kDa, 24.05 kDa and 27.12 kDa, respectively. The theoretical MW of the OsJAZ7-GFP and OsJAZ8-GFP fusion protein, including the linking residue, is 53.80 kDa and 52.31 kDa, respectively. Due to post-translational modifications such as arginine methylation and ubiquitination, the observed band for OsJAZ7-GFP and OsJAZ8-GFP appears slightly higher than the 55 kDa band of the molecular weight marker. **B**, *In vitro* pull-down assay showing the interaction between OsPRMT6a and OsJAZ7. Induced His-OsPRMT6awas incubated with the MBP-OsJAZ7 or MBP protein. Protein samples were immunoprecipitated with anti-His antibodies and immunoblotted with anti-His and anti-MBP antibodies. The symbols ‘‘-’’ and ‘‘+’’ in **A** and **B** denote the absence and presence of the corresponding proteins. **C** and **D**, LCI assay showing the interaction between OsPRMT6a and OsJAZ7 (**C**) (or OsJAZ8 (**D**)) in the leaf epidermal cells of *N. benthamiana*. The pseudocolor bar (right panel) shows the range of luminescence intensity in each image.

Supplementary Figure 9. Arg58 is mono-methylated *in vivo*.

Mass spectrometry analysis showing that fragment of SHQQQQQQGEEELVGLSLAGGRPK peptide contains a mono-methylation in Arg58 residue of OsJAZ1-GFP protein in *p35S:OsJAZ1-GFP/*WT but not in *p35S:OsJAZ1-GFP/osprmt6a-1* transgenic plants.

Supplementary Figure 10. OsPRMT6a methylates arginine residues of OsJAZ7.

A, OsJAZ7 protein sequence showing methylated arginine residues (marked with red font) *in vitro* by mass spectrometry analysis. The blue underlined residues represent the coverage extent of identified protein peptides. **B**, A representative mass spectrometry showing a methylated arginine residue in ATSFAMACSLLSR peptide of OsJAZ7 protein. **C**, A table listing methylated peptides and their methylation modification status detected by mass spectrometry.

Supplementary Figure 11. Expression analyses of *OsJAZ1* in different transgenic lines.
Expression levels of *OsJAZ1* in *p35S:OsJAZ1-GFP/*WT and *p35S:OsJAZ1-GFP/osprmt6a-1* transgenic lines. Those lines chosen for further studies are marked with red. L, independent transgenic line.

Supplementary Figure 12. Spikelet morphologies of *p35S:OsJAZ1-GFP*/WT and *p35S:OsJAZ1-GFP/osprmt6a-1.*
A-**E**, Normal spikelet in *p35S:OsJAZ1-GFP*/WT (L4-8) (**A**) and varied spikelet morphologies including normal spikelet (**B**), and abnormal spikelets with abnormal spikelet structures like long sterile lemma that replaces lemma (**C**), long sterile lemma & spikelet-like (**D**), and only one long sterile lemma and one sterile lemma (**E**) in *p35S:OsJAZ1-GFP/osprmt6a-1*. **F**, *p35S:OsJAZ1-GFP*/WT floret with six stamens, two lodicules, one carpel and two stigmas. The lemma and palea were removed for observation. **G**-**J**, *p35S:OsJAZ1-GFP/osprmt6a-1* produces normal floret like WT (**G**) and abnormal florets with carpel-like (**H**), only two stamen and one lodicule (**I**), and a degenerated spikelet (**J**). le, lemma; pa, palea; sl, sterile lemma; st, stamen; lo, lodicule; stg, stigma; lsl, long sterile lemma; spl, spikelet-like; ca, carpel; cal, carpel-like. Scale bars, 2 mm (**A**-**E**), 1 mm (**F**-**J**).

Supplementary Figure 13. The negative correlation between OsJAZ1 arginine methylation modification and its protein content during rice spikelet development.
Western blot analysis depicting the temporal dynamics of OsJAZ1-GFP protein, and its arginine methylation levels during rice spikelet development. HSP82 was used as a loading control to confirm equal protein loading across lanes. “OsJAZ1-GFP/HSP82” represents the relative OsJAZ1-GFP protein content per unit fresh weight of spikelet. “Methyl/ OsJAZ1-GFP/HSP82” represents the relative arginine methylation modification within the OsJAZ1-GFP protein content per unit fresh weight of spikelet. Spikelets were collected at different

developmental stages as indicated in “Detection of OsJAZ1-GFP protein and arginine methylation levels during rice spikelet development” in Materials and methods section.

Supplementary Figure 14. Higher concentrations of MeJA also promotes OsJAZ1 degradation in the absence of OsPRMT6a.

A, **B**, Western blot analysis reveals that native OsJAZ1 protein and JAZ1-GFP fusion protein in the *osprmt6a-1* mutant background were less susceptible to degradation than those in the WT background under the treatment of 5 mM MeJA.

Supplementary Figure 15. JAs promotes OsJAZ1 degradation in presence of OsPRMT6a.

Confocal scanning images depicting the time course degradation patterns of OsJAZ1-GFP fusion protein in WT and *osprmt6a-1* backgrounds under the treatment of 100 μm MeJA. Scale bar, 40 μm.

Supplementary Figure 16. The arginine methylation of OsJAZ1 does not affect its interaction with OsMYC2 in yeast.

The Y2H assay showing no difference in the interaction between OsMYC2 and OsJAZ1 compared to between OsMYC2 and OsJAZ1 (5K). BD, binding domain; AD, activating domain; the transformed yeast cells were plated on DDO (synthetic dropout /-Trp/-Leu) and QDO (synthetic dropout /-Trp/-Leu/-His/-Ade); the gradients indicate tenfold serial dilutions.

Supplementary Figure 17. Abnormal spikelet morphologies of *oscoi1a oscoi1b* double mutant.

A, Targeted mutation to *OsCOI1a* and *OsCOI1b* by CRISPR/Cas9 technology. Schematic diagram of genomic *OsCOI1a* and *OsCOI1b* is given. Arrows indicate target sites. Exons, Introns and Untranslated regions (UTR) are denoted by black boxes, lines and white boxes, respectively. The panel below shows alignment of WT, *oscoi1a* and *oscoi1b* sequences

containing the CRISPR/Cas9-induced mutated sites. The 18 bp CRISPR/Cas9 target sequences adjacent to the underlined protospacer adjacent motifs (PAMs) are indicated in blue font. **B**-**F**, Normal spikelet in WT (**B**) and varied spikelet morphologies including normal spikelet (**C**), and abnormal spikelets with abnormal spikelet structures like only one long sterile lemma (**D**), glume like (**E**), and two lemmas without palea (**F**) in *oscoi1a oscoi1b* double mutant. **G**, WT floret with six stamens, two lodicules, one carpel and two stigmas. The lemma and palea were removed for observation. **H**-**K**, The *oscoi1a oscoi1b* double mutant produces normal floret (**H**) like WT (**G**) and abnormal florets with lodicule like (**I**), three sterile lemmas (**J**), and a carpel-like (**K**). le, lemma; pa, palea; sl, sterile lemma; st, stamen; lo, lodicule; lol, lodicule like; stg, stigma; lsl, long sterile lemma; gl, glume like; spl, spikelet-like; ca, carpel; cal, carpel-like. Scale bars, 2 mm.

Supplementary Figure 18. The mono-methylation mimic of Arg58 *in vivo* in *p35S:OsJAZ1 (1K)-GFP*/WT transgenic plants is insufficient to affect the spikelet development.

The typical spikelet of the WT exhibits a lemma, a palea, two sterile lemmas, six stamens, two lodicules, one carpel and two stigmas. The lemma and palea were removed partially for observation. *p35S:OsJAZ1 (1K)-GFP*/WT transgenic plants exhibits normal spikelets like WT. Scar bar, 1mm.

Supplementary Figure 19. Abnormal spikelet morphologies induced by *osmyc2*.

A. *OsMYC2* mutation was created using CRISPR/Cas9 technology. The left panel illustrates the schematic structure of *OsMYC2*, with the CRISPR/Cas9 target site indicated by an arrow. Exon and Untranslated region (UTR) are represented by black and white boxes, respectively. The right panel shows a 6-bp deletion in *osmyc2*. The 18 bp CRISPR/Cas9 target sequence adjacent to the underlined protospacer adjacent motif (PAM) indicated in blue font. **B**-**F**, Normal spikelet in WT (**B**) and varied spikelet morphologies including normal spikelet (**C**), and abnormal

spikelets with abnormal spikelet structures like spikelet-like (**D**), long sterile lemma (**E**), and only one spikelet-like structure and two sterile lemmas (**F**) in *osmyc2* mutant.

le, lemma; pa, palea; sl, sterile lemma; lsl, long sterile lemma; spl, spikelet-like. Scale bars, 2 mm (**B**-**F**).

Supplementary Figure 20. The negative correlation between OsJAZ1 arginine methylation and high temperature.

A, **B**, Spikelets of *pUbi:OsPRMT6a-Flag*, *p35S:OsJAZ1-GFP/WT* and *p35S:OsJAZ1-GFP/osprmt6a-1* transgenic plants were sampled in the field at different times with varying temperatures (**A**), or at 10:00 am in different growth chambers with different temperatures (**B**). Both the two analyses show that the relative protein content of OsPRMT6a-Flag and the relative arginine methylation level of OsJAZ1-GFP displays a negative correlation with temperature, while the relative protein content of OsJAZ1-GFP exhibits a positive correlation with temperature in WT background transgenic plants. In contrast, the relative protein content of OsJAZ1-GFP in the *osprmt6a-1* background transgenic plants shows little change at different temperatures.

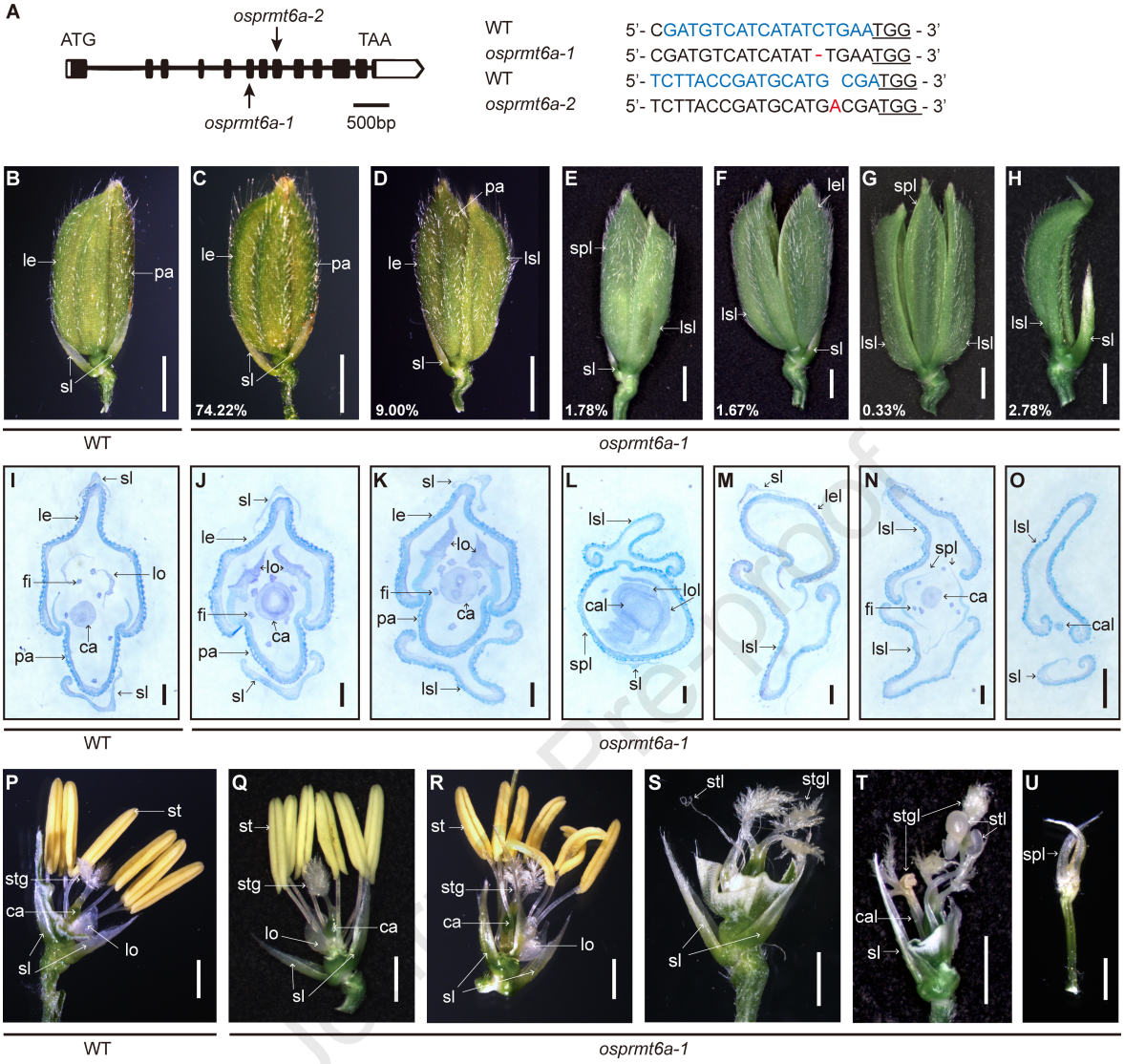

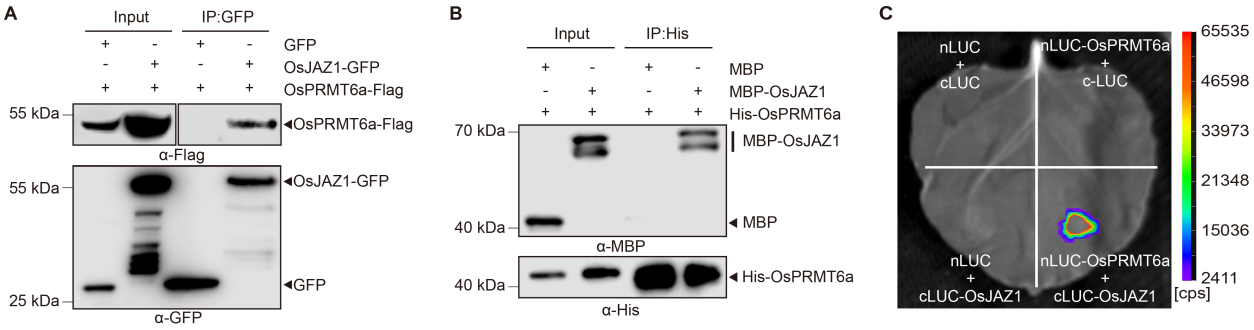

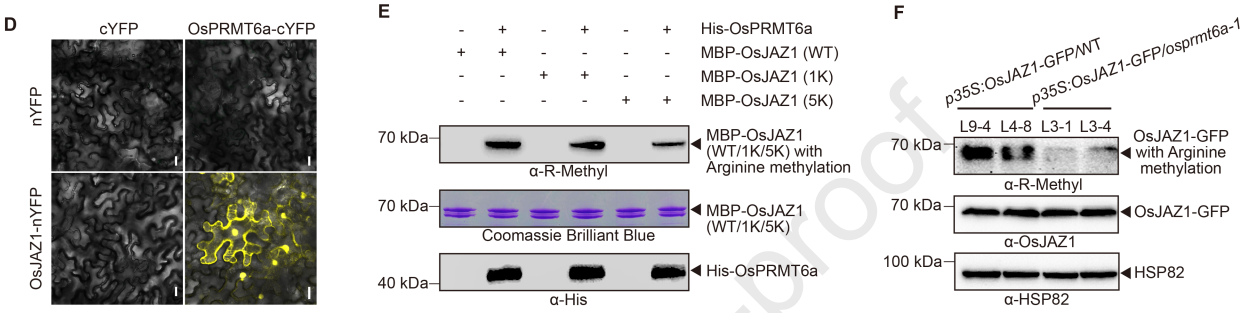

G

MDLLEKKNIKKGGEVEEEVARKGEERKEEEVVVEEK

SHQQQQQQQGEEELVGLSLAGGRPKVFPMSSPPPNP

SQLTIFYGGSVCVYDSVPPEKAQAIMLIAAAAAAAAS

ATKSNAAIAVKPPVMPAANATQAAVSPVLTRSLSLQS

TSVATGQPQVAADPSSICKLQADLPIARRHSLQRFLE

KRRDSRLVSKAPYPTKSSEGMEASGMEVTAEGKAQ*

H

Amino acid	Sequence	Modifications
21R	GGEVEEEVAr	Methyl (+14)
58R	SHQQQQQQQGEEELVGLSLAGGrPK	Methyl (+14)
141R	SNAAIAVkPPVMPAANATQAAVSPVLTr	Dimethyl (+28)
177R	LQADLPIARr	Dimethyl (+28)
191R	DSrLVSkAPYPTk	Dimethyl (+28)

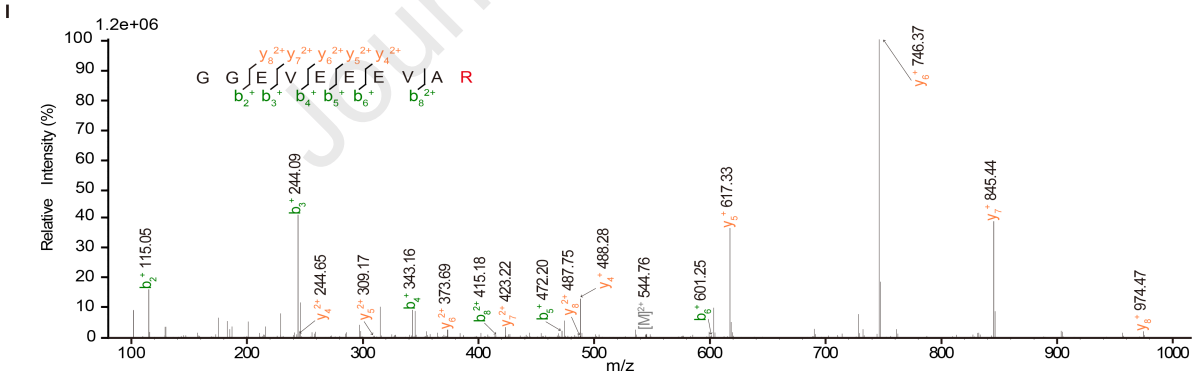

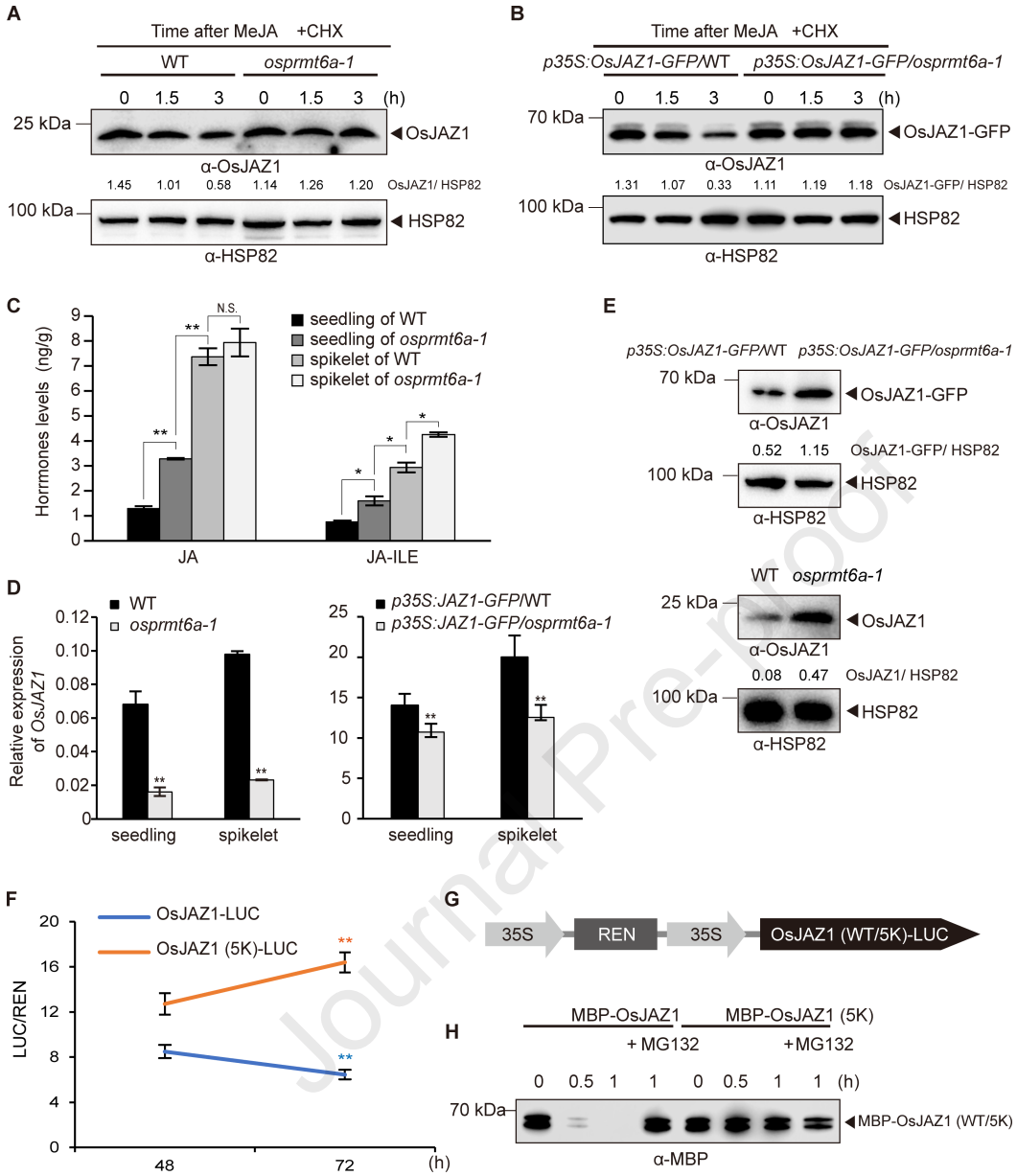
A
Time after MeJA +CHX
WT
osprmt6a-1
0 1.5 3 0 1.5 3 (h)
25 kDa
OsJAZ1
α-OsJAZ1
1.45 1.01 0.58 1.14 1.26 1.20 OsJAZ1/ HSP82
100 kDa
HSP82
α-HSP82
B
Time after MeJA +CHX
p35S:OsJAZ1-GFP/WT
p35S:OsJAZ1-GFP/osprmt6a-1
0 1.5 3 0 1.5 3 (h)
70 kDa
OsJAZ1-GFP
α-OsJAZ1
1.31 1.07 0.33 1.11 1.19 1.18 OsJAZ1-GFP/ HSP82
100 kDa
HSP82
α-HSP82
C
Hormones levels (ng/g)
seedling of WT
seedling of osprmt6a-1
spikelet of WT
spikelet of osprmt6a-1
N.S.
JA
JA-ILE
D
Relative expression of OsJAZ1
WT
osprmt6a-1
seedling
spikelet
p35S:JAZ1-GFP/WT
p35S:JAZ1-GFP/osprmt6a-1
seedling
spikelet
E
p35S:OsJAZ1-GFP/WT p35S:OsJAZ1-GFP/osprmt6a-1
70 kDa
OsJAZ1-GFP
α-OsJAZ1
0.52 1.15 OsJAZ1-GFP/ HSP82
100 kDa
HSP82
α-HSP82
WT osprmt6a-1
25 kDa
OsJAZ1
α-OsJAZ1
0.08 0.47 OsJAZ1/ HSP82
100 kDa
HSP82
α-HSP82
F
OsJAZ1-LUC
OsJAZ1 (5K)-LUC
LUC/REN
48
72
(h)
G
35S
REN
35S
OsJAZ1 (WT/5K)-LUC
H
MBP-OsJAZ1
MBP-OsJAZ1 (5K)
+ MG132
+MG132
0 0.5 1 1 0 0.5 1 1 (h)
70 kDa
MBP-OsJAZ1 (WT/5K)
α-MBP

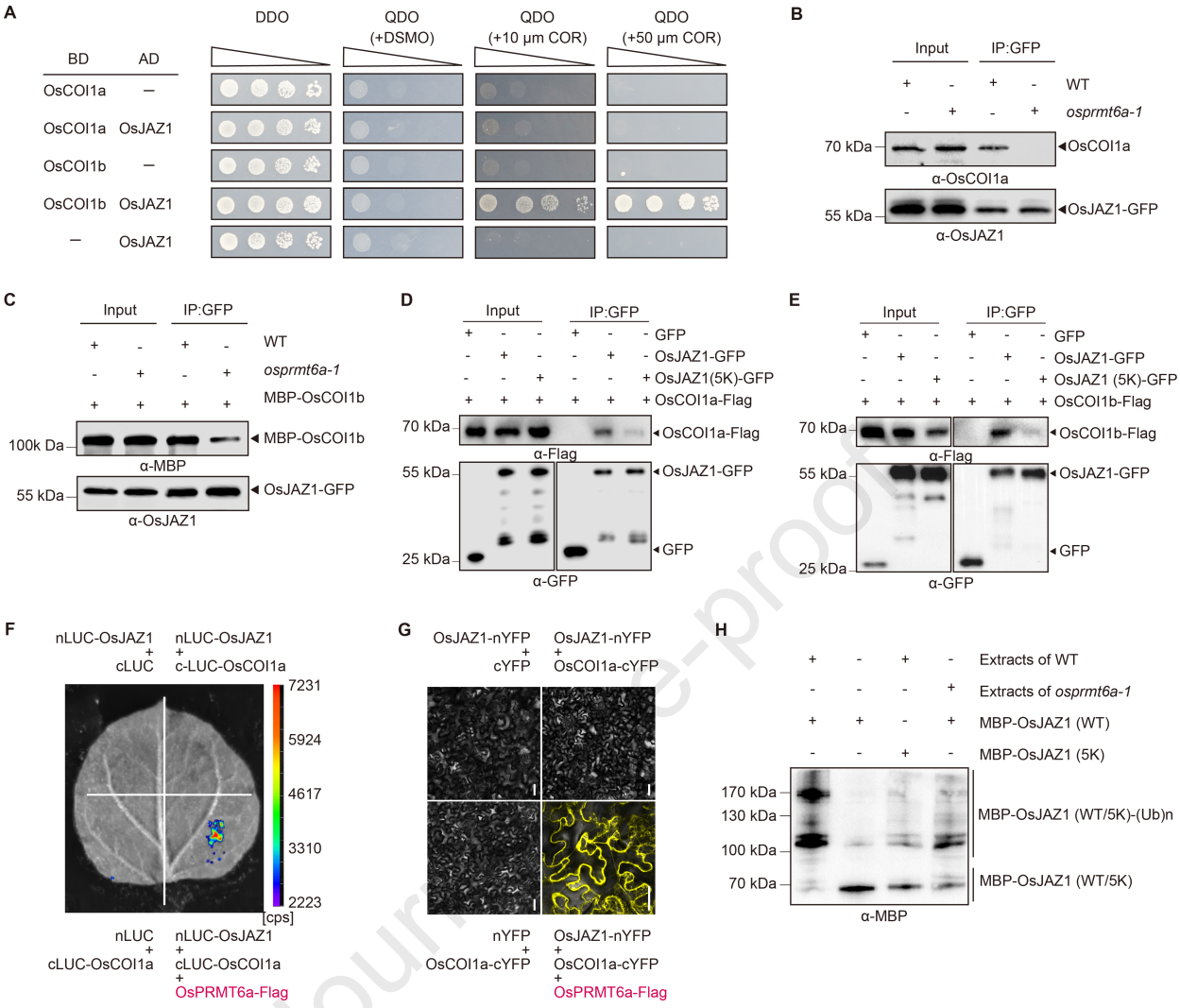
A
DDO
QDO (+DSMO)
QDO (+10 μm COR)
QDO (+50 μm COR)
BD
AD
OsCOI1a
OsCOI1a OsJAZ1
OsCOI1b
OsCOI1b OsJAZ1
OsJAZ1
B
Input
IP:GFP
WT
osprmt6a-1
70 kDa
OsCOI1a
α-OsCOI1a
55 kDa
OsJAZ1-GFP
α-OsJAZ1
C
Input
IP:GFP
WT
osprmt6a-1
MBP-OsCOI1b
100k Da
MBP-OsCOI1b
α-MBP
55 kDa
OsJAZ1-GFP
α-OsJAZ1
D
Input
IP:GFP
GFP
OsJAZ1-GFP
OsJAZ1(5K)-GFP
OsCOI1a-Flag
70 kDa
OsCOI1a-Flag
α-Flag
55 kDa
OsJAZ1-GFP
25 kDa
GFP
α-GFP
E
Input
IP:GFP
GFP
OsJAZ1-GFP
OsJAZ1 (5K)-GFP
OsCOI1b-Flag
70 kDa
OsCOI1b-Flag
α-Flag
55 kDa
OsJAZ1-GFP
25 kDa
GFP
α-GFP
F
nLUC-OsJAZ1 + cLUC
nLUC-OsJAZ1 + c-LUC-OsCOI1a
7231
5924
4617
3310
2223
[cps]
nLUC + cLUC-OsCOI1a
nLUC-OsJAZ1 + cLUC-OsCOI1a + OsPRMT6a-Flag
G
OsJAZ1-nYFP + cYFP
OsJAZ1-nYFP + OsCOI1a-cYFP
nYFP + OsCOI1a-cYFP
OsJAZ1-nYFP + OsCOI1a-cYFP + OsPRMT6a-Flag
H
Extracts of WT
Extracts of osprmt6a-1
MBP-OsJAZ1 (WT)
MBP-OsJAZ1 (5K)
170 kDa
130 kDa
100 kDa
70 kDa
MBP-OsJAZ1 (WT/5K)-(Ub)n
MBP-OsJAZ1 (WT/5K)
α-MBP

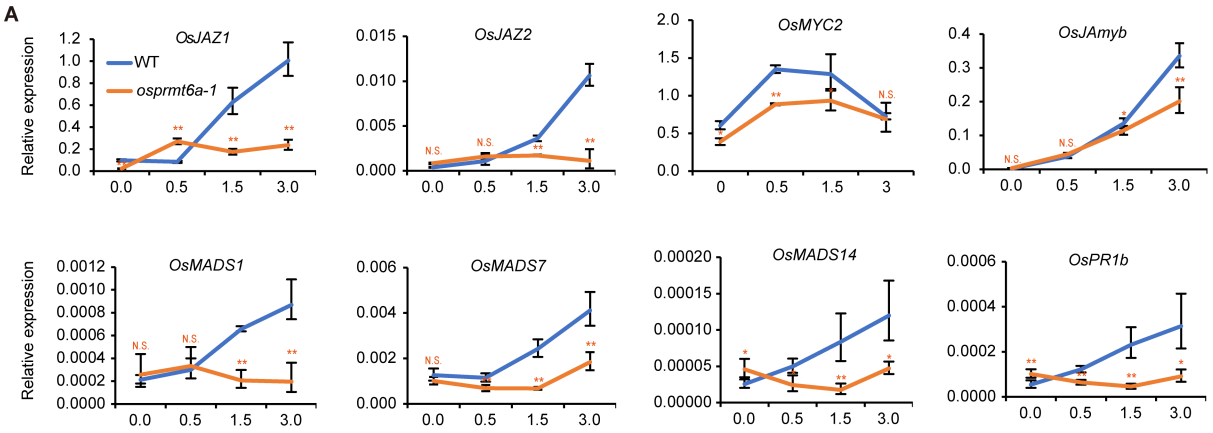
A
OsJAZ1
OsJAZ2
OsMYC2
OsJAmyb
OsMADS1
OsMADS7
OsMADS14
OsPR1b
Relative expression
WT
osprmt6a-1
N.S.

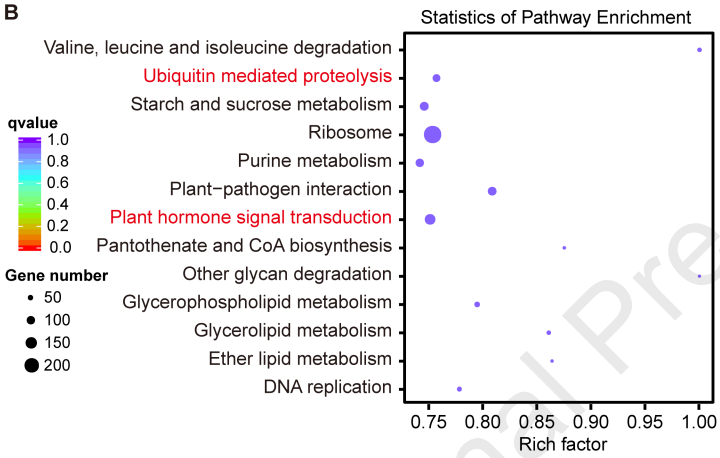
B
Statistics of Pathway Enrichment
Valine, leucine and isoleucine degradation
Ubiquitin mediated proteolysis
Starch and sucrose metabolism
Ribosome
Purine metabolism
Plant−pathogen interaction
Plant hormone signal transduction
Pantothenate and CoA biosynthesis
Other glycan degradation
Glycerophospholipid metabolism
Glycerolipid metabolism
Ether lipid metabolism
DNA replication
qvalue
Gene number
Rich factor

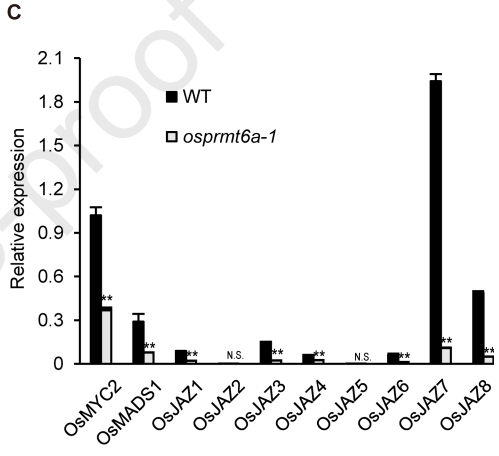
C
WT
osprmt6a-1
Relative expression
OsMYC2
OsMADS1
OsJAZ1
OsJAZ2
OsJAZ3
OsJAZ4
OsJAZ5
OsJAZ6
OsJAZ7
OsJAZ8

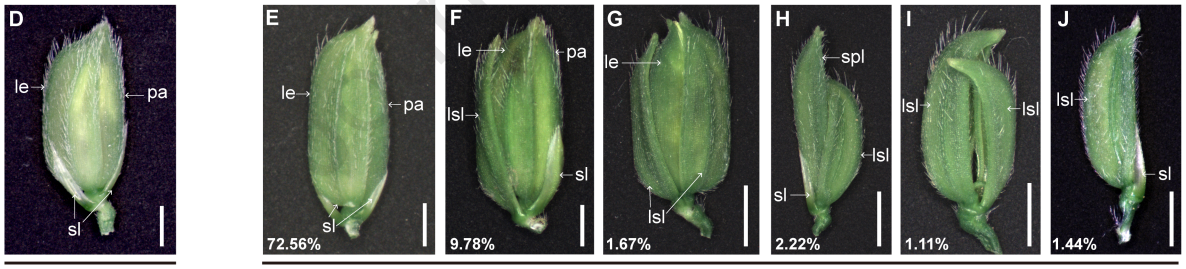
D
E
F
G
H
I
J
le
pa
sl
lsl
spl
72.56%
9.78%
1.67%
2.22%
1.11%
1.44%
WT
p35S:OsJAZ1 (5K)-GFP/WT

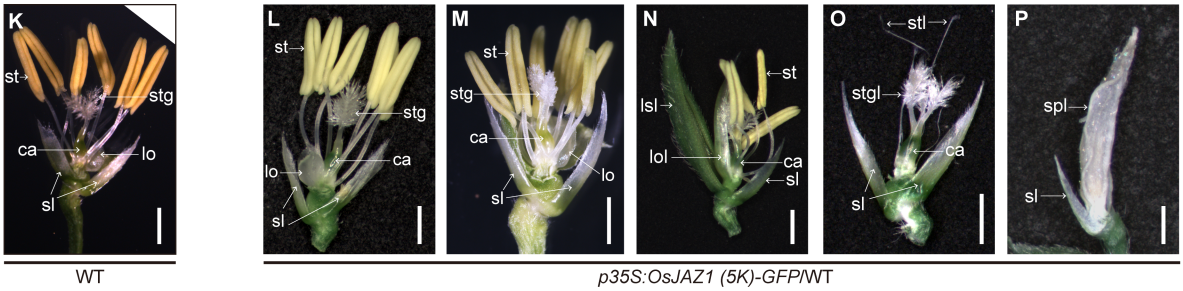
K
L
M
N
O
P
st
stg
ca
lo
lol
stl
stgl
spl
sl
WT
p35S:OsJAZ1 (5K)-GFP/WT

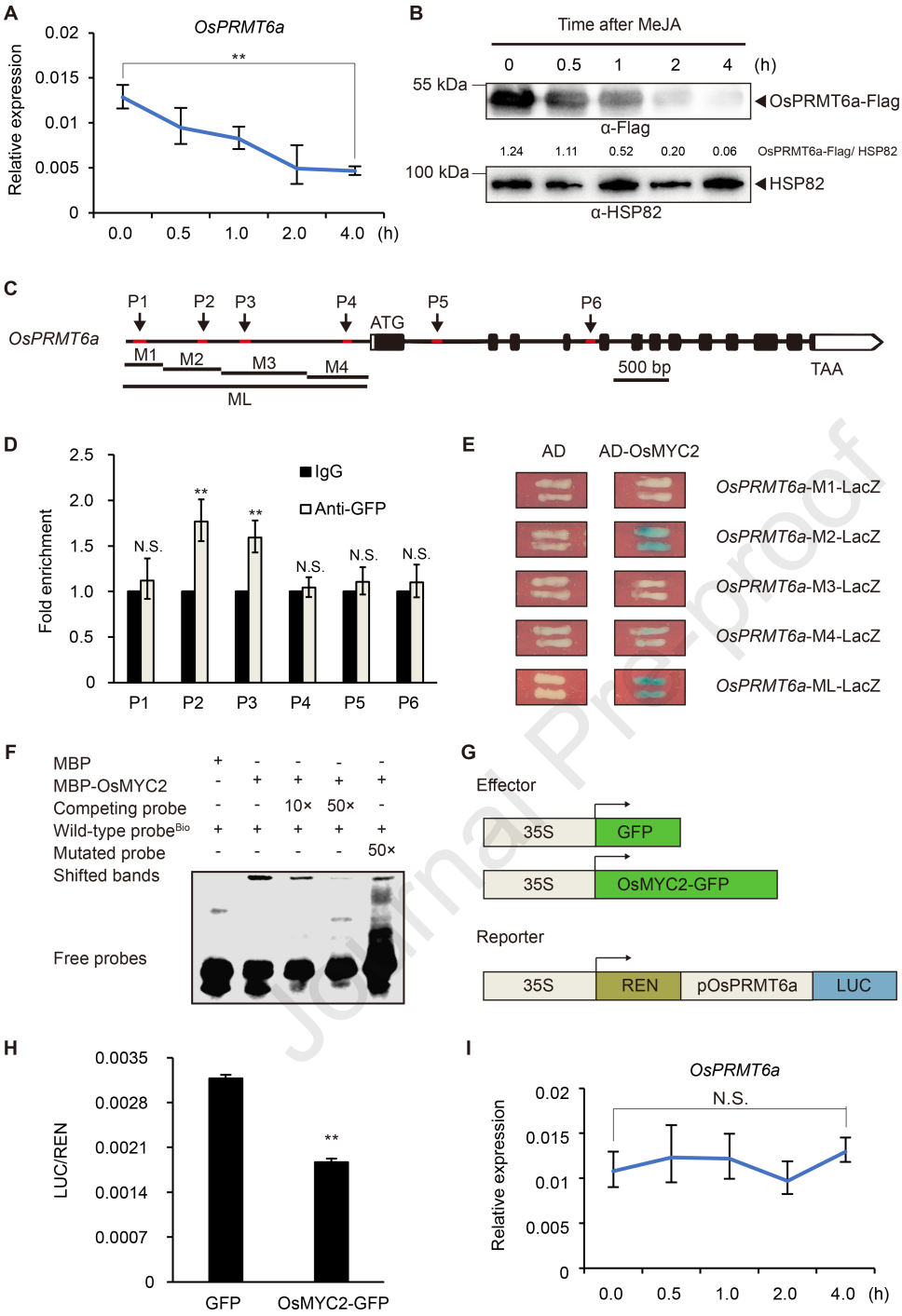

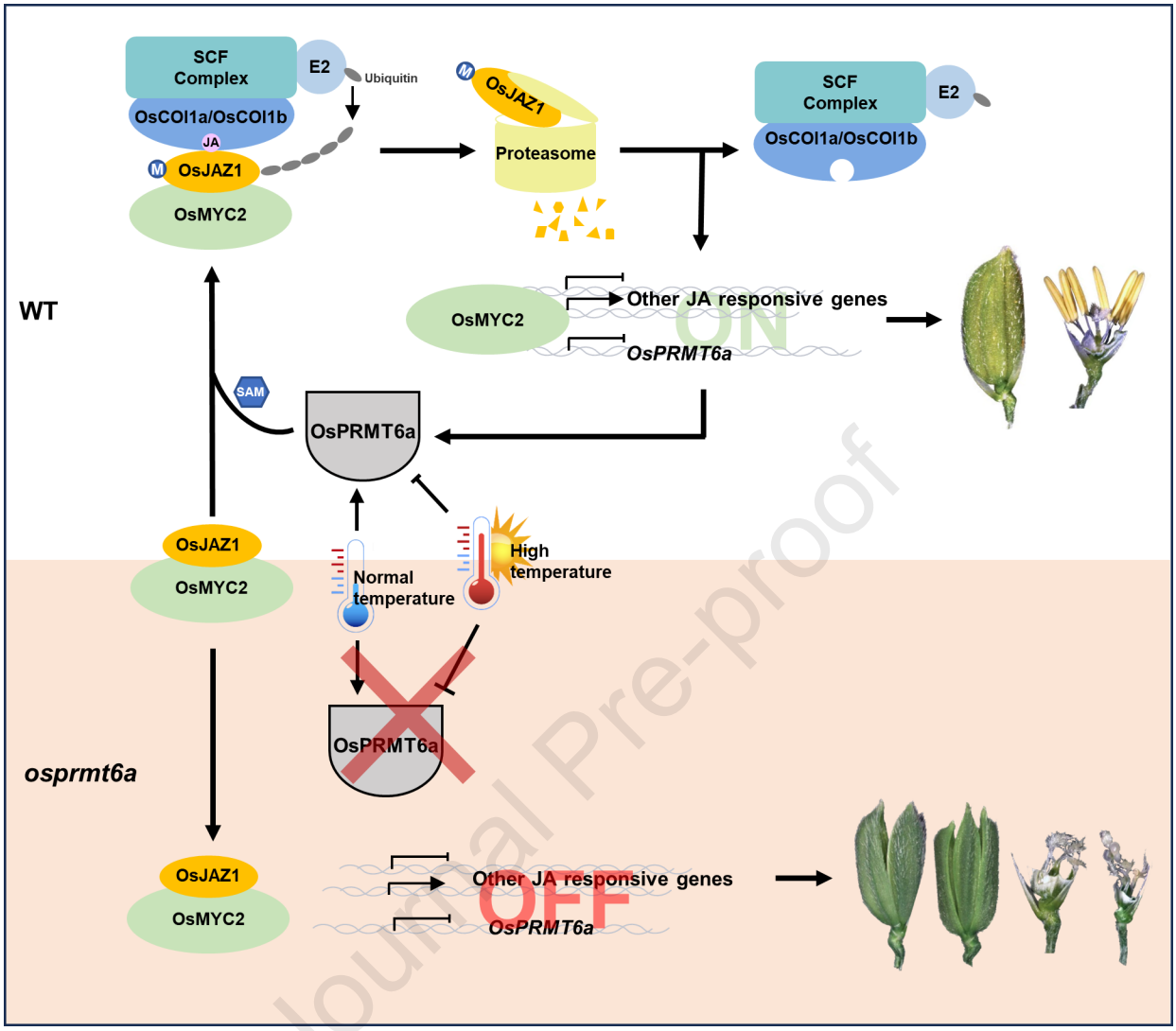

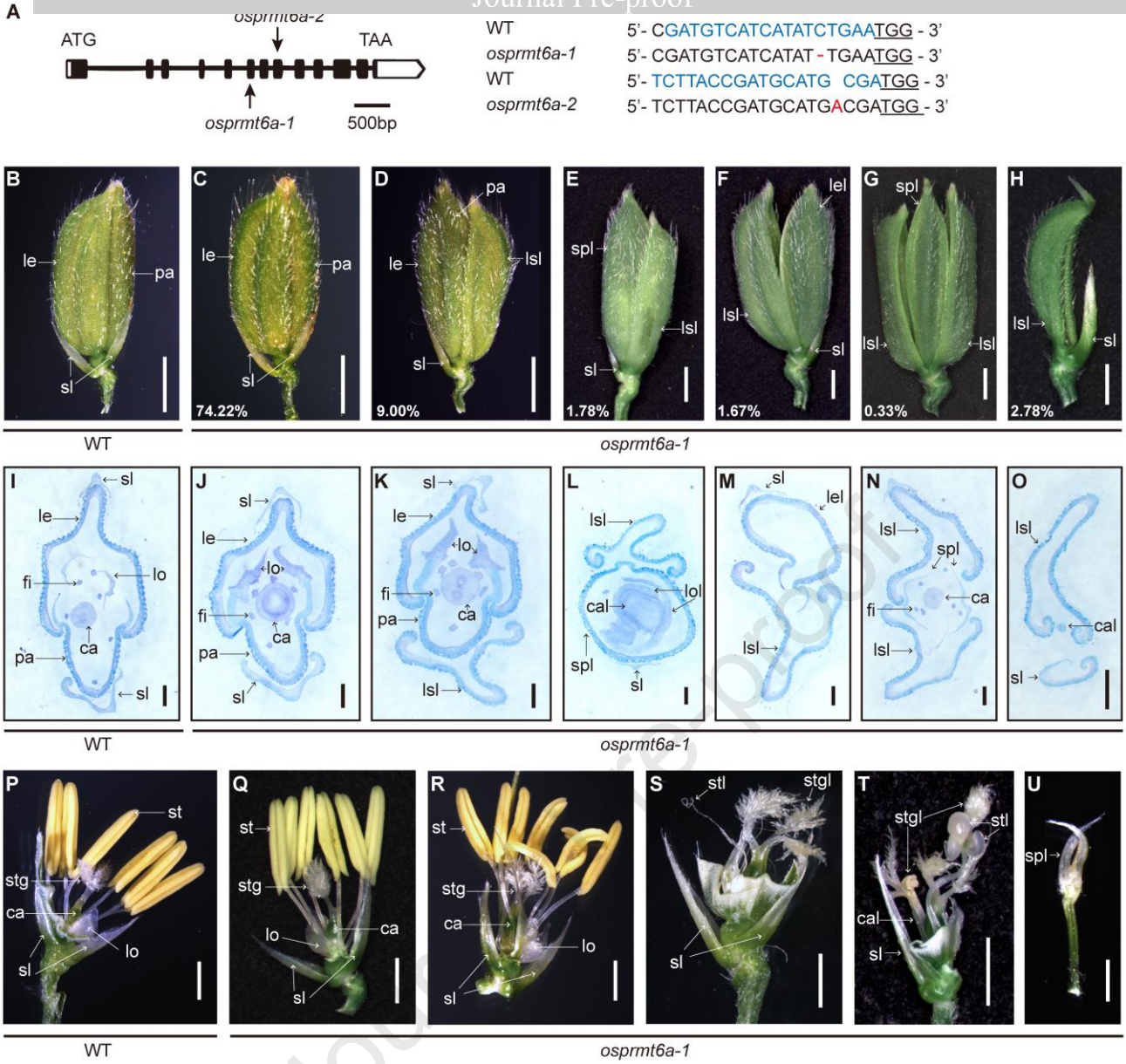

Figure 1. Abnormal spikelet morphologies of *osprmt6a-1* mutant.

A, Targeted mutation to *OsPRMT6a* by CRISPR/Cas9 technology. The diagram shows the genomic structure of *OsPRMT6a*. Arrows indicate target sites. Exons, Introns and Untranslated regions (UTR) are denoted by black boxes, lines and white boxes, respectively. The right panel displays sequence alignment of WT, *osprmt6a-1* and *osprmt6a-2,* highlighting the CRISPR/Cas9-induced mutated sites. Blue font, showing 18 bp CRISPR/Cas9 target sequences adjacent to the underlined protospacer adjacent motifs (PAMs). **B**-**H**, Spikelet morphologies, including normal spikelets in WT (**B**), and various spikelet morphologies in *osprmt6a-1*, consisting of normal spikelet (**C**), and abnormal spikelets with long sterile lemma (**D**), long sterile lemma & spikelet-like (**E**), long sterile lemma & lemma-like (**F**), two long sterile lemmas & spikelet-like (**G**), and one separate long sterile lemma and one sterile lemma (**H**). The ratio of specific mutation type (2020, Shunyi district, Beijing) is marked in the lower left corner. **I**-**O**, Transverse resin semi-thin sections

from **B**-**H**. **P**, WT floret with six stamens, two lodicules, one carpel and two stigmas. The lemma and palea were removed for observation. **Q**-**U**, *osprmt6a-1* produces normal florets like WT (**Q**) and abnormal florets with eight stamens (**R**), three stigmas & stamen-like organ (**S**), severely malformed carpel, stamen, and stigma (**T**), and a degenerated spikelet (**U**). le, lemma; lel, lemma-like; pa, palea; sl, sterile lemma; st, stamen; lo, lodicule; fi, filament; stg, stigma; stgl, stigma-like; lsl, long sterile lemma; spl, spikelet-like; ca, carpel; cal, carpel-like; stl, stamen-like. Scale bars, 2 mm (**B**-**H**), 500 μM (**I**-**O**), 1 mm (**P**-**U**).

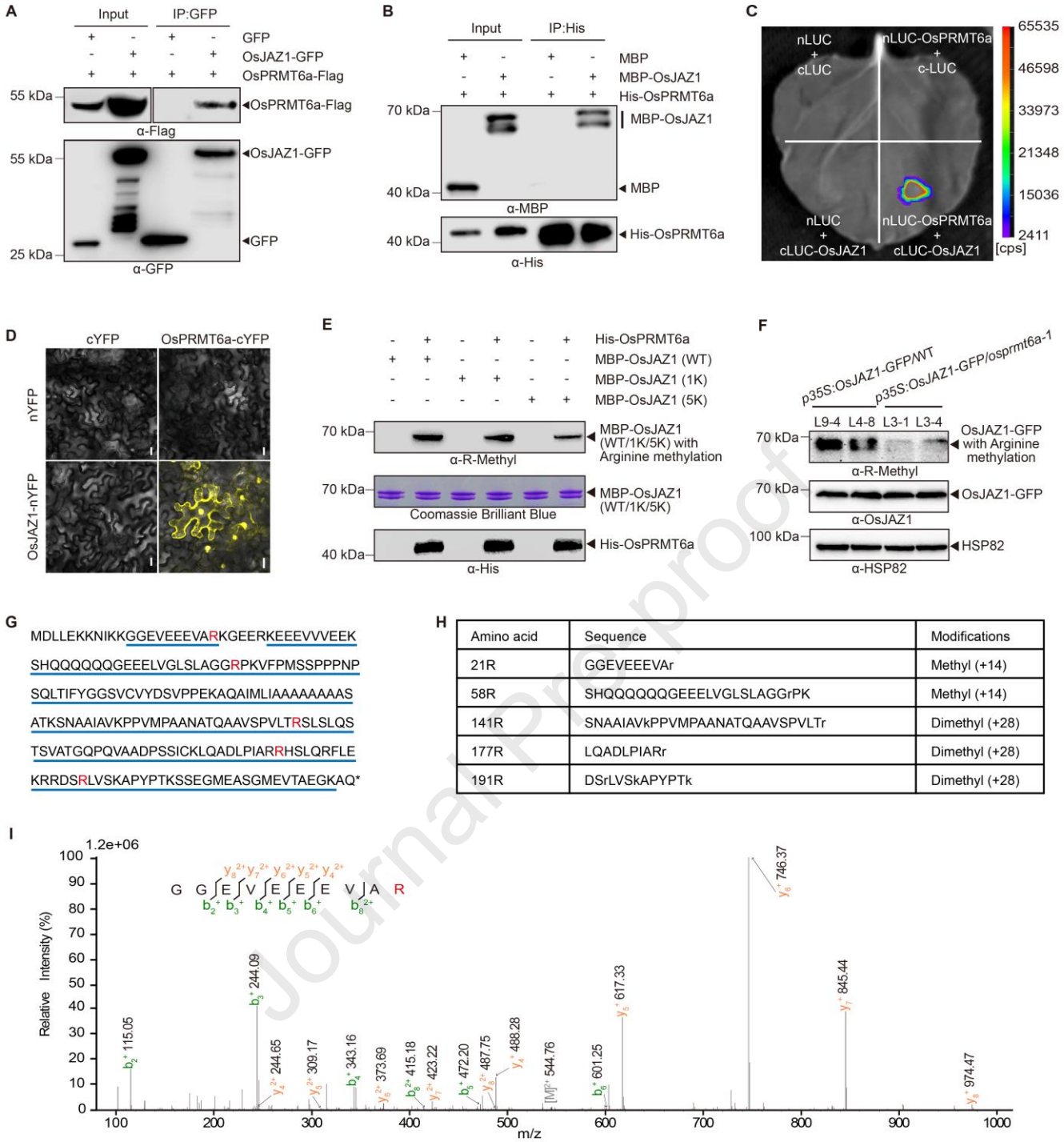

Figure 2. OsPRMT6a physically interacts with OsJAZ1 to methylate arginine residues of OsJAZ1.

A, *In vivo* Co-Immunoprecipitation (CoIP) assay showing the interaction between OsPRMT6a and OsJAZ1 in *N. benthamiana* leaves. The molecular weight (MW) of OsJAZ1 and GFP is 23.02 kDa and 27.12 kDa. The theoretical MW of the OsJAZ1-GFP fusion protein, including the linking residue, is 51.28 kDa. Due to post-translational modifications such as arginine methylation and ubiquitination, the observed band for OsJAZ1-GFP appears slightly higher than the 55 kDa band of the molecular weight marker. **B**, *In vitro* pull-down assay showing the interaction of OsPRMT6a with OsJAZ1. His-OsPRMT6a proteins were incubated with the MBP-OsJAZ1 or MBP proteins. Protein samples were

immunoprecipitated with anti-His antibodies and immunoblotted with anti-His and anti-MBP antibodies. **C**, Luciferase complementation imaging (LCI) assay showing the interaction of OsPRMT6a with OsJAZ1 in *N. benthamiana* leaves. The pseudocolor bar (right panel) shows the range of luminescence intensity in each image. **D**, Bimolecular fluorescence complementation (BiFC) assay showing the interaction between OsPRMT6a and OsJAZ1 in the leaf epidermal cells of *N. benthamiana*. **E**, OsPRMT6a methylated arginine residues of OsJAZ1 *in vitro*. Top and bottom panels, Western blots; middle panel, Coomassie brilliant blue staining. OsJAZ1 (WT/1K/5K) represent the wild-type OsJAZ1, OsJAZ1 with one arginine replaced by lysine and OsJAZ1 with five arginines replaced by lysine, respectively. **F**, OsPRMT6a methylated arginine residues of OsJAZ1 *in vivo*. α-HSP82 shows an equal amount of total proteins, α-OsJAZ1 shows an equal amount of OsJAZ1-GFP protein in the total proteins, and α-R (Arginine)-Methyl shows the levels of methylated arginine residues in OsJAZ1-GFP proteins in plants. **G**, OsJAZ1 protein sequence showing methylated arginine residues (marked with red font) *in vitro* by mass spectrometry analysis. The blue underlined residues represent the coverage extent of identified protein peptides. **H**, A table listing methylated peptides and their methylation modification status detected by mass spectrometry. **I**, A representative mass spectrometry result illustrating a methylated arginine residue in the GGEVEEEVAR peptide of OsJAZ1 protein. Scale bars, 20 μm. The symbols ‘‘-’’ and ‘‘+’’ denote the absence and presence of the corresponding proteins.

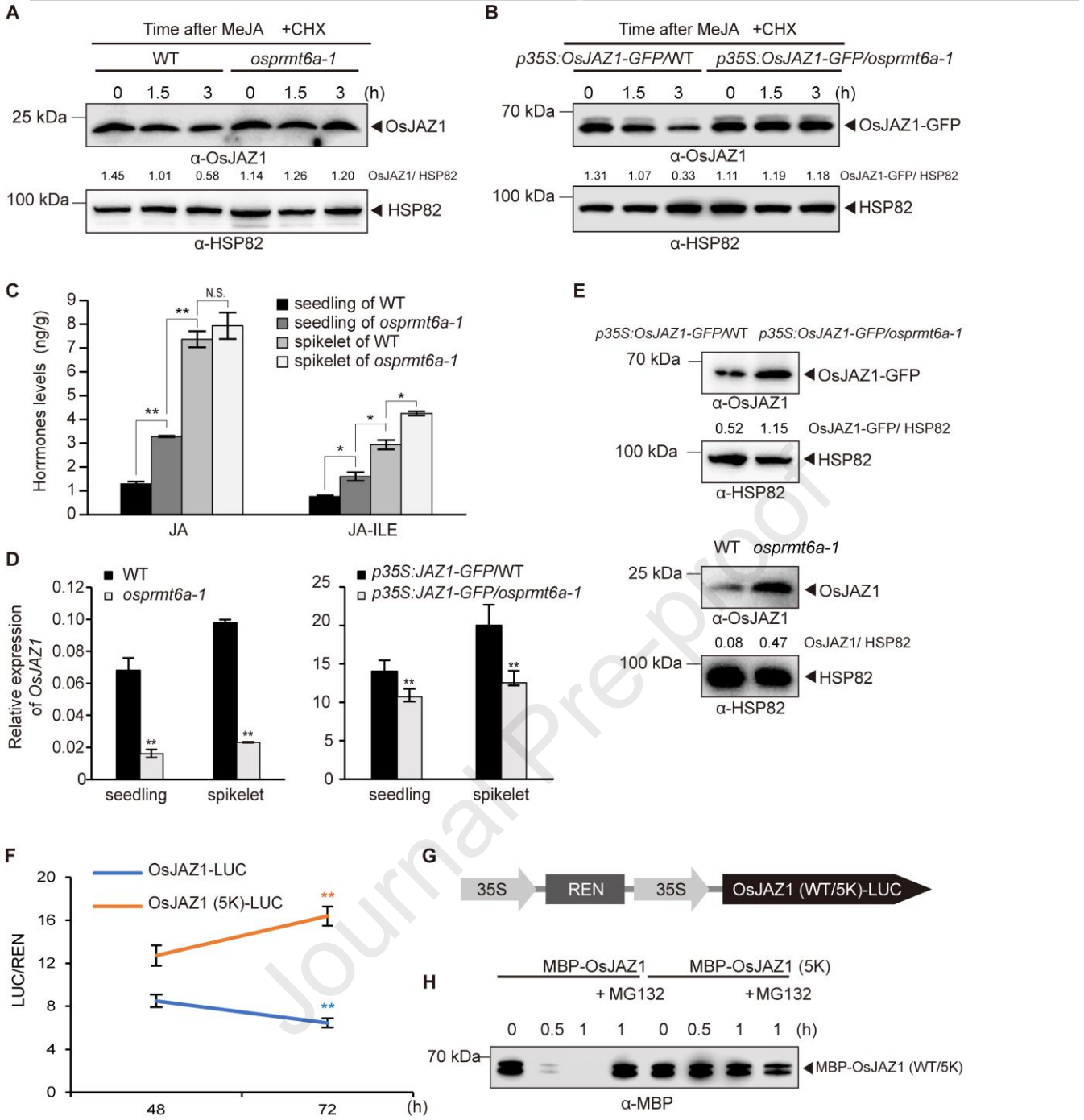

Figure 3. JAs promotes OsJAZ1 degradation in presence of OsPRMT6a.

A, **B**, Western blot analysis reveals that 2 mM MeJA induces the OsJAZ1 degradation in WT but not in *osprmt6a-1*, or the OsJAZ1-GFP degradation in *p35S:OsJAZ1-GFP/*WT but not in *p35S:OsJAZ1-GFP/osprmt6a-1* transgenic plants. **C**, Levels of JA and its amino acid derivative JA-Ile in seedlings and spikelets of WT and *osprmt6a-1*. **D**, Expression levels of *OsJAZ1* in 2-week-old seedlings or spikelets of WT, *osprmt6a-1*, *p35S:OsJAZ1-GFP/*WT and *p35S:OsJAZ1-GFP/osprmt6a-1* transgenic plants. **E**, Protein levels of OsJAZ1 in spikelets of WT and *osprmt6a-1* plants, or OsJAZ1-GFP in spikelets of *p35S:OsJAZ1-GFP/*WT and *p35S:OsJAZ1-GFP/osprmt6a-1* transgenic plants. **F**, *In vivo* dual-LUC-degradation assay using luciferase reporters, OsJAZ1-LUC and OsJAZ1 (5K)-LUC, transiently expressed in *N. benthamiana* leaves for 48 and 72 hours, respectively. Values =

means ± s.e.m. (*n* = 3 replicates). Asterisks, statistically significant differences between samples (*P < 0.05, **P < 0.01 by the Student's t-test). **G**, Schematic representation of the OsJAZ1-LUC and OsJAZ1 (5K)-LUC constructs for the dual-LUC-degradation assay in (**C**). 35S, CaMV35S promoter; REN, Renilla luciferase; OsJAZ1(WT/5K)-LUC, fusion protein of OsJAZ1 (or OsJAZ1 (5K)) and Firefly luciferase. **H**, Cell-free degradation assay shows that MBP-OsJAZ1 is more easily degraded than MBP-OsJAZ1 (5K), and the proteasome inhibitor MG132 inhibits the degradation of MBP-OsJAZ1. Numbers below Western blot images represent the band density ratio of α-OsJAZ1/α-HSP82 (**A**, **B**, **E**), quantified using ImageJ.

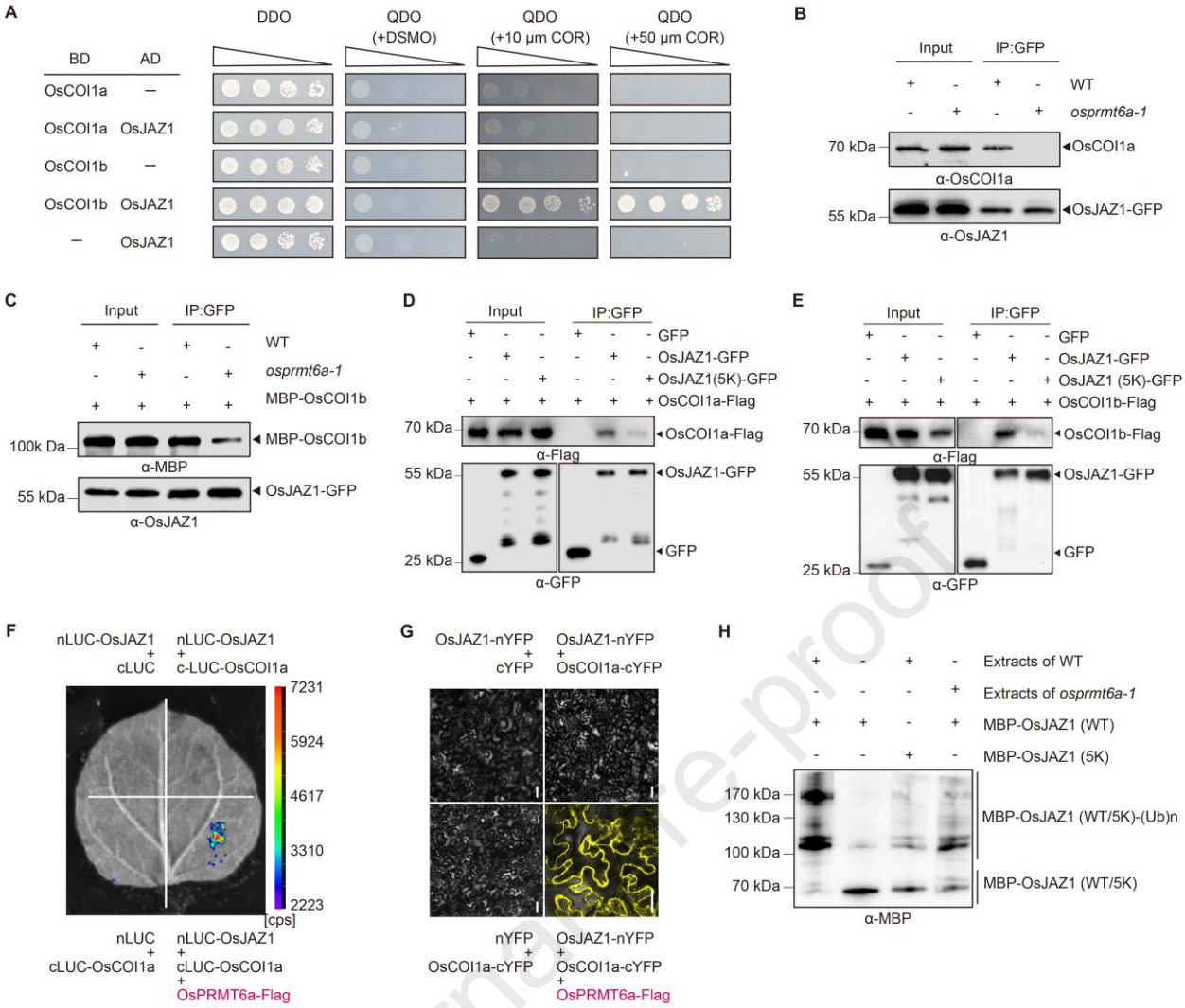

Figure 4. OsPRMT6A promotes the interaction of OsJAZ1 with OsCOI1a or OsCOI1b, and thus its ubiquitination.

A, Y2H assay showing the interaction of OsCOI1b with OsJAZ1 in the presence of COR of different concentrations, no interaction of OsCOI1b with OsJAZ1 in the absence of COR, and no interaction of OsJAZ1 with OsCOI1a in the presence or absence of COR. BD, binding domain; AD, activating domain; the gradients indicate tenfold serial dilutions. **B,** *In vivo* CoIP showing the interaction between OsCOI1a and OsJAZ1-GFP in WT and *osprmt6a-1* background. OsJAZ1-GFP in WT or *osprmt6a-1* were used as bait to immunoprecipitate the native OsCOI1a. **C**, Semi-*in vivo* CoIP showing the interaction between MBP-OsCOI1b and OsJAZ1-GFP in WT and *osprmt6a-1* background. OsJAZ1-GFP in WT or *osprmt6a-1* were employed as bait to immunoprecipitate the exogenously added prokaryotic-expressed MBP-OsCOI1b. **D, E**, *In vivo* CoIP showing the stronger interaction of OsCOI1a-Flag or OsCOI1b-Flag with OsJAZ1-GFP than with OsJAZ1 (5K)-GFP in rice protoplasts. OsJAZ1-GFP or OsJAZ1-GFP (5K) were used as bait to immunoprecipitate the OsCOI1a-Flag or OsCOI1b-Flag. **F**, LCI assay shows that the interaction between OsPRMT6a and OsJAZ1 depends on OsPRMT6a in *N. benthamiana* leaves. The pseudocolor bar (right panel)

shows the range of luminescence intensity in each image. **G**, BiFC assay shows that the interaction between OsPRMT6a and OsJAZ1 depends on OsPRMT6a in the leaf epidermal cells of *N. benthamiana.* **H**, *In vitro* ubiquitination assay showing that OsJAZ1 is more ubiquitinated by WT than by *osprmt6a-1* plant extracts, while OsJAZ1 (5K) exhibits weak ubiquitination by WT plant extracts. Scale bars, 50 μm. The symbols ‘‘-’’ and ‘‘+’’ denote the absence and presence of the corresponding proteins.

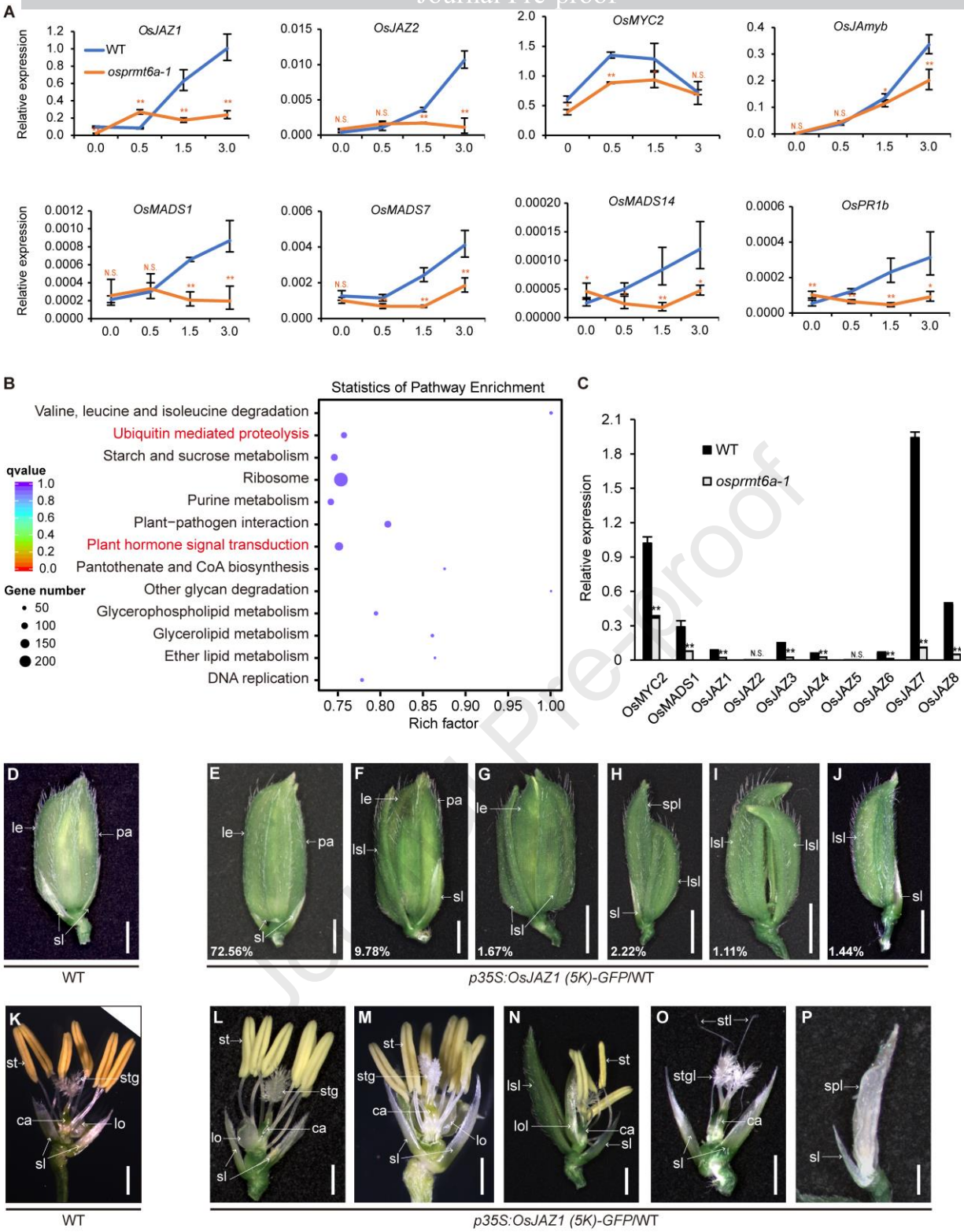

Figure 5. The arginine demethylation status of OsJAZ1 impedes JA responses and normal spikelet development.

A, Expression changes of JA signaling pathway genes. The horizontal axis of the line chart is the sampling time of 25-day-old seedlings after 2 mM MeJA treatment. **B**, RNA-seq analysis of WT vs *osprmt6a-1* DEG enriched KEGG pathway scatter plot. **C**, RT-qPCR results validate the clustering results of RNA-seq about JA signaling pathway. Values are presented as means ± s.e.m. (*n* = 3 replicates). Asterisks represent statistically significant differences in the relative expression of

corresponding genes genes between WT and *osprmt6a-1* at the same time point and “N.S.” denotes no significant (*P < 0.05, **P < 0.01 by the Student’s *t*-test). **D**-**J**, Spikelet morphologies, including normal spikelets in WT (**D**), and various spikelet morphologies like normal spikelet (**E**), abnormal spikelets with long sterile lemma (**F**), two long sterile lemmas (**G**), a long sterile lemma & a spikelet-like structure (**H**), two separate long sterile lemmas (**I**) and one separate long sterile lemma (**J**) in *p35S: OsJAZ1 (5K)-GFP*/WT transgenic plants. The ratio of specific mutation type is marked in the lower left corner. **K**, WT floret with six stamens, two lodicules, one carpel and two stigmas. The lemma and palea were removed for observation. **L**-**P**, *p35S: OsJAZ1 (5K)-GFP*/WT transgenic plants with normal floret like WT (**L**), and abnormal florets with seven stamens (**M**), long sterile lemma & lodicule-like (**N**), three stamens & stigma-like (**O**) or spikelet-like (**P**). Scale bars, 2 mm (**D**-**J**), 1 mm (**K**-**P**). le, lemma; pa, palea; st, stamen; stl stamen-like; sl, sterile lemma; lo, lodicule; stg, stigma; stgl, stigma-like; lsl, long sterile lemma; spl, spikelet-like; ca, carpel; cal, carpel-like; lol, lodicule-like.

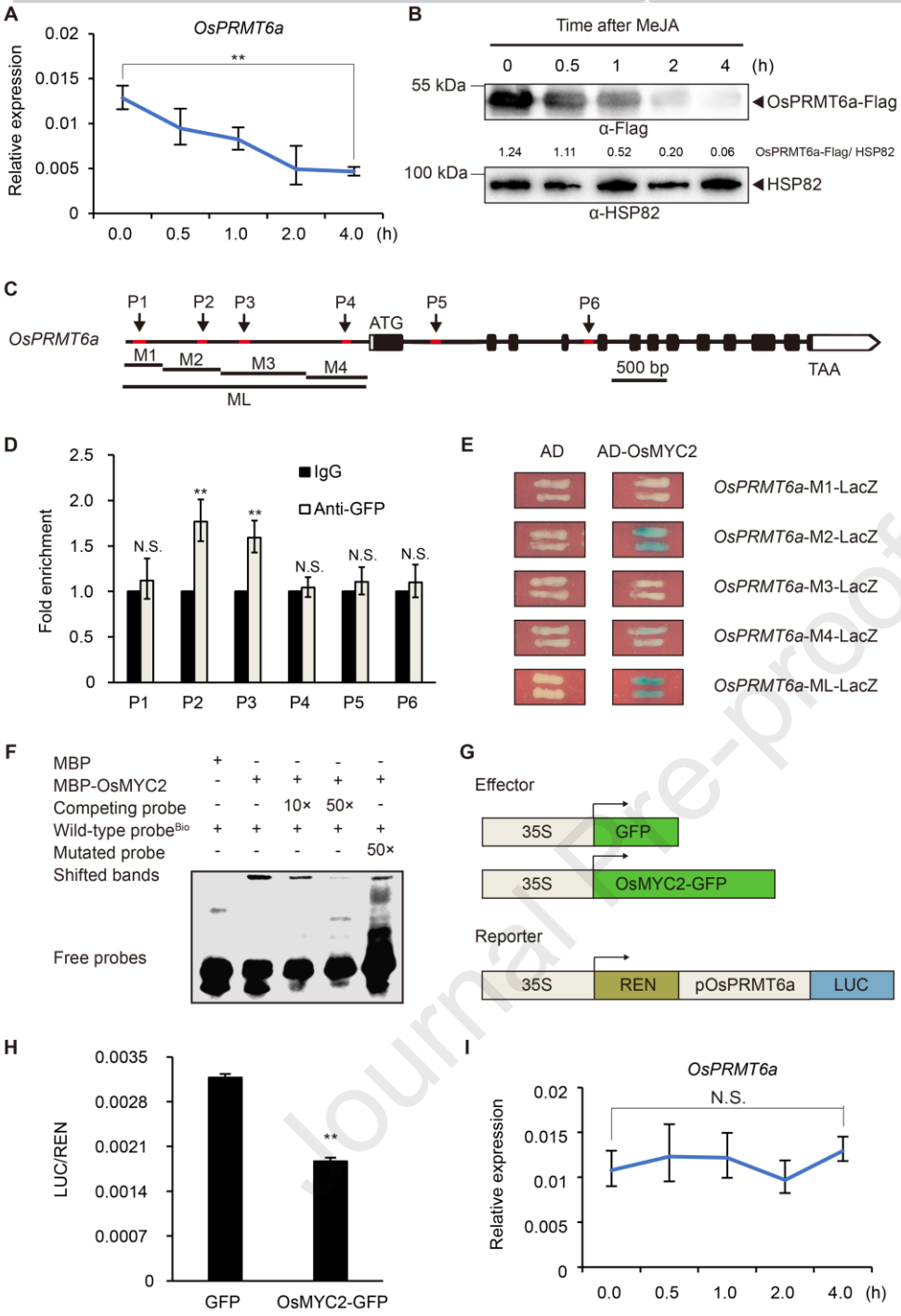

Figure 6. MeJA represses the *OsPRMT6a* expression through OsMYC2.

A, mRNA level of *OsPRMT6a* decreases following 1 mM MeJA treatment in 12-day-old WT seedlings. **B**, Protein level of OsPRMT6a decreases following 1 mM MeJA treatment in 12-day-old *pUbi:OsPRMT6a-Flag* transgenic plants. Numbers below the images represent the band density ratio of α-Flag/α-HSP82 quantified by software ImageJ. **C**, Diagram of the *OsPRMT6a* genomic region featuring DNA fragments (red lines, P1 to P6) with the G-box (5'-CACGTG/CACATG-3') motif. White boxes, untranslated region; black boxes, exons; black lines, introns. **D**, ChIP-qPCR analysis indicating amplification of promoter fragments P2 and P3 from IP pulled down by the anti-GFP antibody. The control, immunoglobulin G was set as 1. **E**, Y1H assays of the binding regions of

OsMYC2 in the promoter regions of *OsPRMT6a*. Series of promoter fragments of *OsPRMT6a* were fused to upstream region of LacZ reporter gene for OsMYC2 binding test. AD, the empty pB42AD, negative control. **F**, EMSA assay showing direct binding of OsMYC2 to the G-box motif in the *OsPRMT6a* promoter. The arrow indicates the shifted band representing the protein–DNA complex. The symbols ‘‘-’’ and ‘‘+’’ denote the absence and presence of the corresponding proteins or probes. **G**, Schematic representation of the effector and reporter constructs. Full-length coding regions of OsMYC2-GFP fusion protein or GFP protein under control of the 35S promoter, as the effectors. The Firefly luciferase gene LUC driven by the *OsPRMT6a* promoters and the Renilla luciferase gene Ren driven by the 35S promoter, as the reporters. **H**, Transient dual-LUC reporter gene assays revealing OsMYC2 inhibition of *OsPRMT6a* transcription. **I**, mRNA level of *OsPRMT6a* in *loss-of-function* mutant *osmyc2* remain relatively unchanged under the treatment of 1 mM MeJA in 12-day-old seedlings. Values are means ± s.e.m. (n = 3 replicates). Asterisks indicate significant differences, and “N.S.” denotes no significant (**P < 0.01 by the Student’s t-test) in **A**, **D**, **H**, **I**.

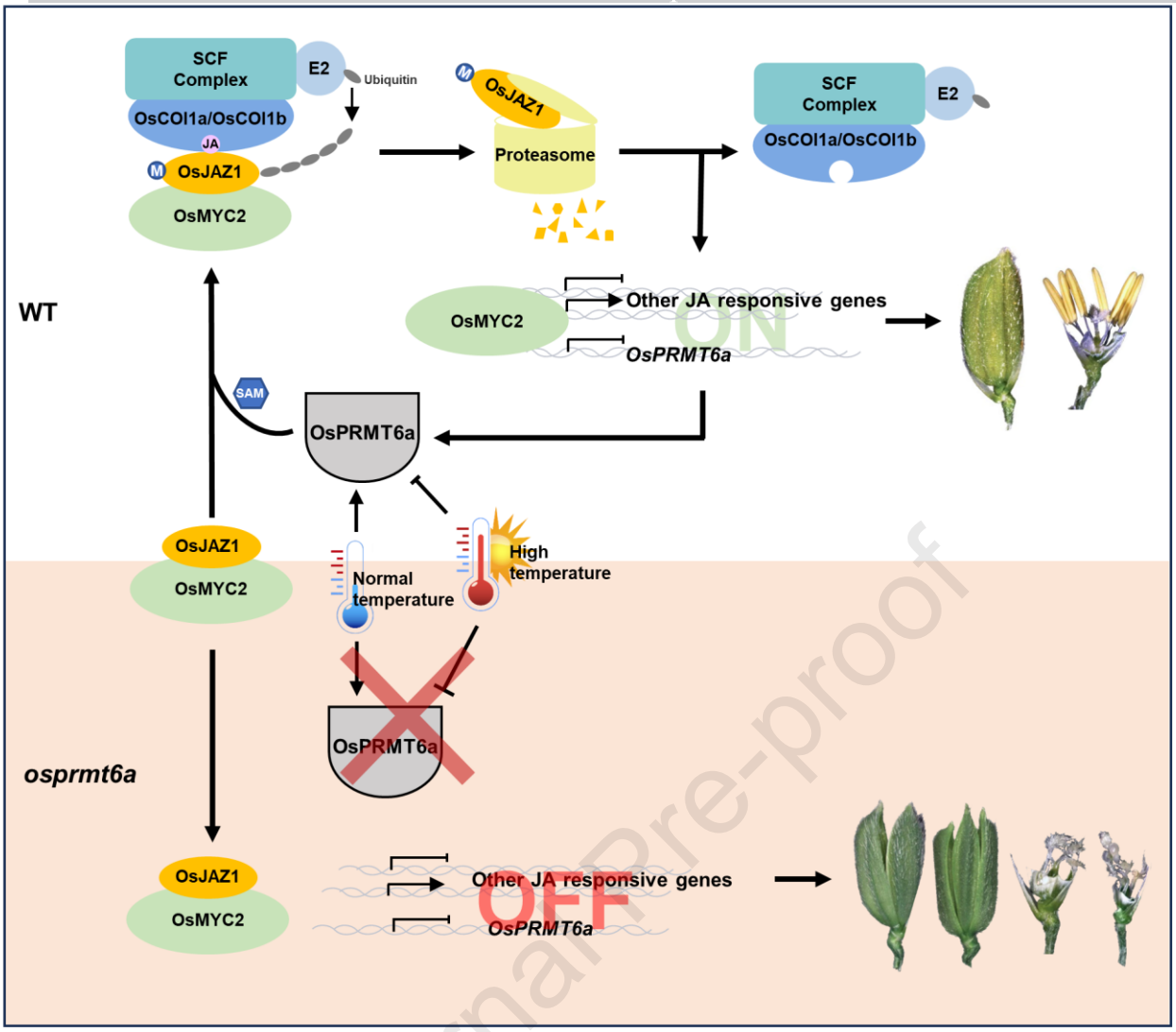

Figure 7. Schematic model depicts that the arginine methylation of OsJAZ1 by OsPRMT6a promotes its degradation and thus JA signal transmit.

In WT, OsPRMT6a methylates arginines of OsJAZ1. The arginine methylation of OsJAZ1 enhances its interaction with OsCOI1a/OsCOI1b, thus promoting the ubiquitination of OsJAZ1 by the $SCF^{OsCOI1a/OsCOI1b}$ complex, subsequently the degradation of OsJAZ1 by 26S proteasome. The degradation of OsJAZ1 frees OsMYC2 to activate (or repress) JA-responsive genes, including *OsPRMT6a*, ultimately promoting the transmission of the JA signal to maintain normal spikelet development. And the OsPRMT6a protein accumulates at normal temperatures but decreases at high temperatures, leading to dynamic changes in OsPRMT6a-regulated arginine methylation and protein level of OsJAZ1 with temperature fluctuations. SAM, methyl donor S-adenosylmethionine. M, methyl.

However, in *loss-of-function osprmt6a* mutants, the dynamic changes of OsPRMT6a-regulated arginine methylation and protein level of OsJAZ1 are not observed, leading to the constant stabilization of OsJAZ1. This stabilization hinders JA signaling transduction, ultimately causing abnormal spikelet development.